Atypical integrative element with strand-biased circularization activity assists interspecies antimicrobial resistance gene transfer from *Vibrio alfacsensis*

Lisa Nonaka,[1,2*] Michiaki Masuda,[1] Hirokazu Yano[3,4,† *]

[1]Department of Microbiology, Dokkyo Medical University School of Medicine, Mibu, Tochigi, Japan

[2]Faculty of Human Life Sciences, Shokei University, Kumamoto, Japan

[3]Faculty of Life and Environmental Sciences, University of Tsukuba, Tsukuba, Japan

[4]Graduate School of Life Sciences, Tohoku University, Sendai, Japan

† Current address: Antimicrobial Resistance Research Center, National Institute of Infectious Diseases, Higashimurayama, Japan

Short title: Integrative elements with strand-biased circularization activity

*Corresponding authors

Email: nonaka20@shokei-gakuen.ac.jp (LN); h-yano@niid.go.jp (HY)

Abstract

The exchange of antimicrobial resistance (AMR) genes between aquaculture and terrestrial microbial populations has emerged as a serious public health concern. However, the nature of the mobile genetic elements in marine bacteria is poorly documented. To gain insight into the genetic mechanisms underlying AMR gene transfer from marine bacteria, we mated a multidrug-resistant *Vibrio alfacsensis* strain with an *Escherichia coli* strain, and then determined the complete genome sequences of the donor and the transconjugant strains. Sequence analysis revealed a conjugative multidrug resistance plasmid in the donor strain, which was integrated into the chromosome of the recipient. The plasmid backbone in the transconjugant chromosome was flanked by two copies of a 7.1 kb unclassifiable integrative element harboring a β-lactamase gene. The 7.1 kb element and the previously reported element Tn*6283* share four coding sequences, two of which encode the catalytic R-H-R-Y motif of tyrosine recombinases. Polymerase chain reaction and sequencing experiments revealed that these elements generate a circular copy of one specific strand without leaving an empty site on the donor molecule, in contrast to the movement of integron gene cassettes or ICE/IMEs discovered to date. These elements are termed SEs (strand-biased circularizing integrative elements): SE-6945 (the 7.1 kb element) and SE-6283 (Tn*6283*). The copy number and location of SE-6945 in the chromosome affected the antibiotic resistance levels of the transconjugants. SEs were identified in the genomes of other *Vibrio* species. Overall, these results suggest that SEs are involved in the spread of AMR genes among marine bacteria.

Introduction

Antimicrobials have been used globally in aquaculture to control fish diseases. Although this approach helps to maintain a stable supply of aquacultural products, misuse of antimicrobials has led to the emergence of antimicrobial-resistant microbes and the accumulation of resistance genes at aquaculture sites [1,2]. As the spread of multidrug-resistant (MDR) bacteria and pan-drug-resistant bacteria threatens human life [3,4], it is important to obtain clues about whether and how aquatic and terrestrial microbial populations exchange genetic materials.

Conjugative plasmids [5] and integrative and conjugative elements (ICE) [6] are DNA units that can move from one cell to another through the conjugation machinery that they encode. They can directly move between species [7,8], and indirectly mobilize genes on specific mobile elements [9–11]. Plasmids can be classified into families according to the replicon type or the mobilization machinery type for epidemiological purposes [12,13].

Transposons have been defined as specific DNA segments that can repeatedly insert into one or more sites in one or more genomes [14]. Several distinct strand exchange mechanisms and the routes used for their location changes, i.e., *transposition*, have been discovered to date [15]. In a comprehensive review by Curcio and Derbyshire [15], transposons were classified into five families based on the DNA strand exchange enzymes used. In prokaryotes, the mode of transposition was largely classified into ‘cut-out paste-in’ (often called ‘excision integration’ for the ICEs [6]), ‘copy-out paste-in,’ or ‘copy-in’ for which replication is necessary to complete transposition; e.g., Tn*3*, IS*91*. DNA insertion involving DNA replication can also be seen in the integration of integron gene cassettes into *attI* [16] and the phage CTX into *dif* [17]; both use tyrosine recombinase(s) as the strand exchange

enzyme. In transposon classification, ICEs are classified as transposons that use a Y-transposase (tyrosine recombinase) or an S-transposase (serine recombinase) [15]. Other than ICEs, DNA segments that can move to a location in other cells via the excision – transfer (rolling-circle replication) – integration route have been termed IME (integrative mobilizable element) [18], MGI (mobilizable genomic island) [19], CIME (*cis*-mobilizable element) [20], or MTn (mobilizable transposon) [21] (hereafter collectively referred to as IME). IMEs encode site-specific recombinase or DDE transposase as strand exchange enzyme [22]. They have been recognized as degraded forms of ICEs [20]. ICEs/IMEs so far studied in the laboratory seem to change their location via the 'excision integration' route only [23–26]. Genes embedded in these mobile genetic elements are readily shared among bacteria and provide genetic resources for microbial adaptation in changing environments.

To better understand the genetic mechanisms underlying the spread of antimicrobial resistance (AMR) genes at aquaculture sites, we previously collected resistant bacteria from sediments at an aquaculture site in Kagawa, Japan [27–29]. We identified a self-transmissible MDR plasmid of the MOB_H-family, named pAQU1, that can replicate in both the original host *Photobacterium damselae* subsp*. damselae* and in *Escherichia coli* [28]. Subsequently, another MOB_H-family MDR plasmid, named pSEA1, was identified in a *Vibrio alfacsensis* isolate (previously identified as *V. ponticus*) [30]. pSEA1 carries a 12 kb unclassifiable integrative element, Tn*6283*, in addition to the AMR genes. Although pSEA1 could not replicate in *E. coli* at 42 °C, following conjugation, it could cointegrate with the *E. coli* chromosome by homologous recombination between two Tn*6283* copies: one on pSEA1 and another that moved from pSEA1 into the chromosome [30]. Further, Tn*6283* was suggested to circularize one specific strand without producing an empty site, presumably

using tyrosine recombinases. However, it is not known whether interspecies gene transfer assisted by Tn*6283*-like elements is common in nature.

To obtain further insights into the mechanisms behind genetic exchange among aquaculture-associated bacteria, in this study we mated another MDR *Vibrio* isolate, *V. alfacsensis* 04Ya249, with *E. coli* strains in the laboratory and then determined the genome sequences of both the donor and transconjugant strains. We identified a Tn*6283*-like element involved in the cointegration of the multidrug resistance plasmid and the *E. coli* chromosome. Based on the findings in the previous study and this study, we have termed Tn*6283* and a related element as a new class of mobile elements: strand-biased circularizing integrative element (SE). Tn*6283* is hereafter referred to as SE-6283.

In this study, several types of intracellular DNA movement need to be discussed. For clarity, the terms *transposition*, *cointegration*, and *integration* are used here based on the following rules. We call the movement of a DNA segment from one location to the other location in one or two genomes, mediated by any DNA strand exchange enzymes, transposition. The physical incorporation of a plasmid into a chromosome is called cointegration regardless of the molecular mechanisms and genomic locations involved. The physical incorporation of a DNA molecule into a specific site in another molecule mediated by a site-specific recombinase (so-called integrase) is called integration.

Results

Identification of SE carrying a β-lactamase gene

We previously isolated *V. alfacsensis* strain 04Ya249 from sea sediment at an aquaculture site [27]. 04Ya249 showed resistance to erythromycin, tetracycline, and ampicillin [31]. To

111 identify active mobile elements in this strain that are relevant to its AMR, the strain was
112 mated with macrolide-sensitive *E. coli* JW0452, and transconjugants were selected on
113 erythromycin at 42 °C. One transconjugant was named strain TJ249.

114 The complete genome sequences of strains 04Ya249 and TJ249 were determined
115 using the PacBio RS II platform. The genome of strain 04Ya249 consists of four replicons:
116 two chromosomes, a 306 kb putative conjugative plasmid pSEA2, and an 82 kb putative
117 conjugative plasmid pVA249. Strain 04Ya249 has a very similar genome architecture to the
118 database strain *V. alfacsensis* CAIM 1831 based on gene synteny (S1 Fig A) and average
119 nucleotide identity (S1 Fig B). Seven AMR genes were identified on pSEA2 (S2 Fig A). One β-
120 lactamase gene (60 % product identity to bla_{VHH-1} in the CARD database [32]) was located
121 within a 7.1-kb repeat region found in both chromosome 1 and pSEA2 (S2 Fig B). This β-
122 lactamase gene has been assigned a new family name, bla_{GMA} (Gammaproteobacterial
123 Mobile Class A β-lactamase), and allele name, bla_{GMA-1}, in NCBI.

124 The chromosome of *E. coli* TJ249 contains two notable insertions (Fig 1 A), a smaller
125 insertion of the 7.1-kb element alone immediately downstream of the putative transcription
126 termination site for *yjjN* (*yjjNt*) located between *yjjN* and *yjjO* (in GenBank accession no.
127 U00096.3), and a larger insertion into *insJ* of IS*3*, containing a nearly complete copy of pSEA2
128 and an additional copy of the 7.1 kb element. These indicate the movement between
129 different genomic locations (pSEA2, *yjjNt*, *insJ*), thereby transposition, of the 7.1 kb element
130 in *E. coli*. Thus, the 7.1 kb element was labelled a transposon and assigned a four digit
131 identifier, 6945, by the transposon registry [33] . As the 7.1-kb element was confirmed to
132 generate a circular copy of one specific strand without leaving an empty site like SE-6283 in
133 this study (see below), the 7.1 kb element was regarded as a new SE and designated SE-
134 6945.

As pSEA2 showed > 99.9 % nucleotide identity in the aligned region to pSEA1 (accession no. LC081338.1) from strain 04Ya108 [30], we also determined the complete genome of strain 04Ya108 for comparison with strain 04Ya249. As predicted from Southern hybridization [30], strain 04Ya108 possessed two copies of SE-6283, one in chromosome 1 and the other in plasmid pSEA1. Strain 04Ya108 also carries two copies of SE-6945, in the same locations on the chromosome and plasmid as strain 04Ya249 (S1 Fig A, S2 Fig B). The four coding sequences in SE-6945 showed homology to the four coding sequences clustered at one end of SE-6283 (Fig 1 B). The biochemical functions of the products of the four genes were predicted using Pfam and InterProScan in EMBL. The *intA* and *intB* products generated a hit on phage_integrase (CL0382) in Pfam and were further aligned with known tyrosine recombinases using structure-aware alignment program PROMAL3D [34] to confirm the presence of conserved motifs. The *intA* and *intB* products contained the catalytic R-H-R-Y motif (G-R motif in box I and H-R-H-Y motif in box II (Fig 1C)) conserved in tyrosine recombinases [35], though the N-terminal region of IntB is extraordinarily long among tyrosine recombinases. CDS2 and CDS4 products did not generate hits in the Pfam or InterProScan databases. SE-6283 and SE-6945 carry imperfect 19 bp inverted repeat motifs at their ends (Fig 1 B), termed C and C' based apparent on functional equivalence to the core-type sites of phages [36]. Gene product identities between the SE-6945 and SE-6283 counterparts were 22.5 % for IntA, 20.5 % for CDS2, 23.2 % for IntB, and 26.6 % for CDS4 in blastp.

Fig 1. Genetic features of SEs.

(A) Schematic representation of the 7.1 kb element and pSEA2 insertion locations in *E. coli* TJ249. Yellow pentagons are the 7.1 kb element. The sequence from pSEA2 is indicated by a

horizontal line. (B) Upper panel: Genetic organization of SE-6283 and SE-6945. Lower panel: Nucleotide sequences of imperfect inverted repeat motifs C and C'. Dots indicate that bases in C are identical to those in C'. (C) Presence of R-H-R-Y motif in IntA and IntB. IntA and IntB sequences are aligned with sequences of known tyrosine recombinases based on secondary structure prediction using PROMAL 3D [34]. The aligned regions corresponding to box I and box II in [35] are shown.

The border regions between SE-6945 and its target locations were termed *attL* (*intA*-proximal side) and *attR* (*intA*-distal side) (Fig 2 A). The nucleotide sequence alignments of *attL* and *attR* from the two *E. coli* chromosomal locations and the two locations in 04Ya249 genomes (pSEA2 and chr 1) are shown in S3 Fig and S4 Fig, respectively. Sequence comparison of the *attL*, *attR*, and unoccupied target site in the host (*attB*) in *E. coli* (Fig 2 B) revealed that the 6 bp next to the 3' end of C' in *attR* in *E. coli* (5'-TTTTCT-3') was identical to the 6 bp next to the 5' end of C at *attL* on pSEA2, while the 6 bp next to the 5' end of C in *attL* (5'-TTCTTT-3' in *insJ*, 5'-TTTTTT-3' in *yjjNt*) was from *attB* (S3 Fig, S4 Fig, Fig 2 B). Therefore, SE-6945 inserts itself, ending with 5'-GTA-3' (Fig 1 B) along with an additional 6 bp next to the 5' end of C at *attL* on the donor molecule into the target site. The 6 bp from the donor molecule is placed next to the 3' end of C' in the newly formed *attR.*

Target site preference of SE-6945 and SE-6283

After the isolation and genome sequence determination of TJ249, additional mating experiments between *E. coli* JW0452 and *V. alfacsensis* 04Ya249 were performed to test whether pSEA2 insertion into a specific location in the *E. coli* chromosome accompanying

182 SE-6945 transposition is reproducible. Independent mating was performed more than 17
183 times, and transconjugants were screened on tetracycline (Tc) alone, ampicillin (Ap) alone,
184 or both Ap and Tc. The SE-6945 integration pattern was investigated by Southern
185 hybridization for 16 randomly chosen Tc resistant transconjugants, and one Tc sensitive but
186 Ap-resistant transconjugant obtained from selection with Ap alone (S5 Fig C). Among 16 Tc
187 resistant transconjugants, 12 strains had *intA* at the *yjjNt*-SE-6945 junction or the *insJ*-SE-
188 6945 junction. These 16 strains also generated pSEA2-derived fragments (S5 Fig C). The
189 remaining four strains generated pSEA2-derived fragments and contained only one copy of
190 *intA*, suggesting SE-6945-independent pSEA2 cointegration with the chromosome;
191 autonomous replication of pSEA2 seems unlikely given the high frequency of pSEA2
192 cointegration with the chromosome in other transconjugants. Strain LN52, obtained from
193 selection with Ap alone, carried only one SE-6945 copy, and it was integrated into *yjjNt* (S5
194 Fig A, C). Taken together, these observations suggest that pSEA2 integration relies on SE-
195 6945 transposition, and that SE-6945 prefers *yjjNt* or *insJ* of IS*3*, rather than random sites in
196 the *E. coli* genome.

197 To obtain further insights into the target site of SE-6945, bacterial genomes carrying
198 SE-6945 were searched for based on blastn in the NCBI nucleotide collection (nr/nt)
199 database using the SE-6945 core gene region (*intA*-CDS2-*intB*-CDS4) as the query. The
200 genome of *Vibrio harveyi* strain WXL538 contains a segment showing 88.9% nucleotide
201 sequence identity to SE-6945 core genes. Genome structure comparisons between WXL538
202 and 04Ya249 revealed that WXL538 carries a 16.4 kb SE-6945-like SE (provisionally termed
203 SE-VhaWXL538) containing a different set of cargo genes (Fig 2 A). SE-VhaWXL538 is
204 integrated into the promoter region of a *yaaA* gene encoding an H_2O_2_YaaD_Superfamily
205 protein (NCBI conserved domain accession no. cl01143) (locus_tag F9277_14400 in

CP045070.1). This location corresponds to the SE-6945 insertion location in *V. alfacsensis* chromosome 1 (Fig 2 A). Sequences of-target sites (*attB*) in *E. coli*, *V. alfacsensis*, and *V. harveyi* are shown in Fig 2 B. The conservation level of nucleotides in *attB* is presented in Fig 2 C as sequence logo information contents [37]. The central 6 bp putative crossover region in *attB* ~~was~~ is T rich. However, other motifs, such as imperfect inverted repeat structures observed in *attC/attI* of integrons (IntI target) [38,39], or *dif* of CTX phage integration site (XerC/XerD target) [17], could not be detected in *attB, attL* (S3 Fig), or *attR* (S4 Fig) for SE-6945 in the current data set.

Fig 2. Locations of SE-6945 and its related elements.

(A) Comparisons of genetic organization around SE insertion locations. GenBank accession numbers (*Vibrio* strains only) and the coordinates of genomic segments compared are shown below the strain name. (B) Alignment of *attB* sequences. The sequences are retrieved from SE-free genomes. Since the SE-6945-free pSEA2 ancestor could not be found in the database, the bases in the putative crossover region could not be defined and are shown as x. Nicking is expected to take place next to the central box: position is shown by black arrowhead. (C) Sequence logo representation of conservation levels of *attB* sequence.

We previously reported SE-6283 integration into the *bcp* gene encoding peroxiredoxin (locus_tag b2480) in *E. coli.* SE-6283 also carries a *bcp* homolog (locus_tag VYA_19800 in AP024165.1) as if it complements the disrupted *bcp* gene in the host genome upon insertion [30]. Genome sequencing of strain 04Ya108 in this study revealed that one SE-6283 copy was integrated into a *bcp* gene homolog in chromosome 1 (Fig 3 A). To obtain further insight into the target site preference of SE-6283, SE-6283-like elements in public

databases were screened for using blastn. SE-6283-like SEs were identified in three other *Vibrio* species (Fig 3 A). The sizes of SE-6283 and related SEs ranged from 13.8 kb (SE-6283) to 41.3 kb (SE-ValK09K1 in Fig 3 A). Although the motifs C and C′ of the three SE-6283-like elements were slightly different from those of SE-6283 (see *attL* in S6 Fig and *attR* in S7 Fig), all are integrated into *bcp* orthologs in chromosome 1: chromosome 1 (or I) of *V. alginolyticus* strain K09K1 is incorrectly named as chromosome II in CP017919. Comparison of *attL*, *attR*, and unoccupied *attB* found in the SEs-free genome of each *Vibrio* species suggests the integration of SE-6283-like elements and the 6 bp sequence into the central 6 bp putative crossover region in *attB* (Fig 3 B). Nucleotide sequences around putative nicking sites in *attB* for SE-6283 are G and A-rich and, like *attB* of SE-6945 did not possess an inverted repeat structure (Fig 3 C). These observations collectively suggest that, like ICEs, SEs target a few selected locations.

Fig 3. Location of SE-6283 and its related SEs.

(A) Comparisons of genetic organization around SE elements in five genomic locations. GenBank accession numbers and the coordinates of genomic segments compared are shown below the strain name. Except SE-6283 on pSEA1, all elements are integrated into a *bcp* gene and carry a *bcp* gene. (B) Alignment of *attB* sequences from different bacterial species. (C) Sequence logo showing conservation levels of *attB*. The arrowhead indicates the putative nicking site on the top strand.

Transposition of SE-6945 aids pSEA2-chromosome cointegration

The direct repeat structure of SE-6945 in the TJ249 chromosome suggested that pSEA2 was integrated into the recipient chromosome through the transposition of SE-6945, with subsequent cointegration of pSEA2 with the chromosome by homologous recombination between SE-6945 copies: one on the chromosome and the other on pSEA2 (referred to as a two-step gene transfer mechanism in the previous study [30]). If this scenario holds, integration of SE-6945 alone should occur more frequently than pSEA2-chromosome cointegration upon mating, and the cointegration would be reduced in frequency or abolished altogether in a *recA*-null mutant recipient. To test these possibilities, we conducted additional mating assays.

Quantitative mating assays were performed using a rifampicin-resistant recipient strain, JW0452rif, and its isogenic strain carrying *recA* deletion JW0452Δ*recA*rif. Note that Tc resistance is on pSEA2, while Ap resistance is on SE-6945. The transfer of Tc Ap resistance from *V. alfacsensis* 04Ya249 to *E. coli* JW0452rif was detected only in 2 out of 4 replicated mating experiments, and the transfer frequency was determined to be approximately 10^{-9} per donor, indicating a very rare event, generating 0–3 transconjugant colonies per mating (Fig 4). The transfer of Ap resistance alone was observed at >300-fold higher frequency than the transfer of both Tc and Ap resistance (compare the first and the second groups from left in Fig 4), indicating that integration of SE-6945 alone occurs more frequently than pSEA2-chromosome cointegration during mating.

The transfer of Tc Ap resistance to JW0452Δ*recA*rif could not be detected in any of the four independent mating assays (below detection limit of 1.02×10^{-9} per donor).

Unexpectedly the mean transfer frequency of Ap resistance to JW0452Δ*recA*rif was about 17-fold lower than that to JW0452rif (compare the second and the fourth groups from the left in Fig 4). Thus, the direct effect of *recA* knockout on the cointegration could not be evaluated due to the reduced detection sensitivity of gene transfer. However, the mean transfer frequency of Tc Ap resistance to LN52rif (which already carries one copy of SE-6945 and wild type *recA*) was about 56-fold higher than that to JW0452rif (compare the first and fifth groups in Fig 4). This indicates that the presence of the 7.1 kb long identical sequence in both target DNA and pSEA2 promotes cointegration of pSEA2 and the recipient chromosome.

Tn*3*-like cointegrate formation [15] might happen if SE-6945 could simultaneously introduce nicks at one site on the top strand at *attL* (or *attR*) and one site on the bottom strand at *attR* (or *attL*), and DNA-protein crosslink (DPC) repair [40] could clean the linked tyrosine recombinase to produce a 3′-OH priming site. If SE-mediated cointegrate formation occurs, then Tc Ap-resistant transconjugants should emerge at a comparable frequency to Ap-resistant transconjugant, which was not the case in our observation.

Collectively, these results and the nature of tyrosine recombinases support the model that pSEA2-chromosome cointegration mainly occurs through a two-step gene transfer mechanism, transposition followed by homologous recombination, rather than through a one-step Tn*3*-like cointegrate formation process.

Fig 4. Resistance gene transfer from *V. alfacsensis*.

Transfer frequency (Y-axis) is the $\log_{10}$-transformed value of the transconjugant colony-forming units (CFU) divided by the donor CFU. Four replicate mating experiments were performed. No transconjugants were detected in any of the four replicate experiments using

297 JW0452Δ*recA*rif with Tc Ap selection or in the two replicate experiments using JW0452rif
298 with Tc Ap selection (indicated by open circles placed at the bottom). In one experiment on
299 LN52rif, the donor CFU was not evaluated, but the transconjugant CFU was obtained at a
300 comparable frequency to that observed in the other three replicate experiments. The
301 detection limit of this experiment was around 1.02×10^{-9} per donor.
302

303 **Strand-biased circularization of SE-6945**

304 We previously [30] revealed the following unique features of SE-6283: (i) it does not
305 generate an unoccupied donor site upon circularization *in vivo*, and (ii) the circular form of
306 SE-6283 is generated using only one strand as a template at least in *E. coli*. We note that
307 this assertion is based on the notion that tyrosine recombinases generally do not produce
308 blunt ends at *att* sites on double stranded DNA during strand exchange. Although SE-6283
309 encodes tyrosine recombinases and not a single DDE transposase, the outcomes described
310 above, which result only from a figure-eight structure containing a single stranded DNA
311 bridge (Path 1 in Fig 5 A), is reminiscent of the first step of the 'copy-out paste-in'
312 transposition of some ISs [41] (IS*3* route), rather than the excision of ICEs (ICE/IME route) or
313 the generation of circular integron gene cassettes by *attC* × *attC* recombination (gene
314 cassette route) [25,42,43]. If the figure-eight structure containing a single stranded DNA
315 bridge is subject to replication without DPC repair, the products would be a single stranded
316 SE circle, the original copy of donor molecule, and the nicked chromosome, which is
317 eventually lost (Fig 5 A bottom left). To test whether circular copy production of SE-6945
318 also follows Path 1, we created a pSEA2-free 04Ya249 derivative strain LN95 carrying only a

single copy of SE-6945 in the chromosome (S5 Fig B) and analyzed the production of its circular molecule in this strain and the sequence of strand exchange products.

Pairs of primers were designed such that one primer anneals inside the integrative element and the other outside it (Fig 5 A), amplifying *attL* (*intA* side, Fig 5 B, product size 304 bp), *attR* (*bla* side, 248 bp), empty donor site (*attB,* 345 bp), occupied *attB* (7.4 kb), and *attS* (joint of motif C and C' formed on the circular SE-6945, 206 bp). Primer set '1-4' in Fig 5 A was used to detect both empty *attB* and occupied *attB*.

The circular form of SE-6945 was detected in LN95 (Fig 5 B(i)) as well as the parent strain 04Ya249 (S8 Fig A). This suggests that the chromosomal copy of SE-6945 in *V. alfacsensis* is functional. The empty *attB* (345 bp) could not be detected under PCR conditions with short extension times (Fig 5 B(i)), while a larger product of occupied *attB* (7.4 kb) was detected when long PCR conditions were used (Fig 5 B(ii)).

Fig 5. PCR and sequencing analyses of SE-6945 circle.

(A) PCR experiment to detect SE-6945 circle. Upper panel: primer annealing locations (triangles in gray) on SE-6945 and the *attB* region. The number corresponds to the primer set numbers in B. Primer number indicates the following primers in Table 2: 1, LN_181_attB_L; 2, LN_142_junction2; 3, LN_143_junction2; 4, LN183_attB_R2. Lower panel: possible routes of SE movement. Two strands of DNA are shown as separate lines, with SE in orange. In Path 1 (solid arrows), one strand is nicked, and the SE side is circularized while the host DNA side of the strand remains not joined, leading to a figure-eight structure containing a single stranded DNA bridge. The figure-eight form can be subject to replication, giving rise to a double stranded SE circle (if the recombinase bound 3' end is cleaned, for example, by DPC repair [40], referred to as 'IS*3* (copy-out) route'), or single stranded DNA

circle (if the 3' end is not cleaned). In Path 2, strand exchange generates a figure-eight containing a double stranded DNA bridge. After going through Path 2, there are two possible outcomes: (i) another round of strand exchange at bottom strand leading to a circular double stranded SE as well as a circular donor molecule carrying empty donor site ('ICE/IME route'), (ii) replication on the figure-eight leading to single stranded SE circle and donor molecule with empty *attB*, and the original donor molecule ('gene cassette route'). (B) The result of PCR. PCR products were electrophoresed in 2% agarose gel (i) or 0.8% agarose gel (ii). (C) Putative nicking sites in *attL* and *attR*. The SE DNA is shown in orange. Nicking and ligation at positions shown as arrowheads in the same color can generate *attS* with a 6 bp spacer. (D) Observed *attS* sequences. *attS* type 1 can be generated from strand exchange at the top strand on chromosome 1 or bottom strand on pSEA2, while *attS* type 1 can be generated from strand exchange at the top strand on pSEA2 or bottom strand on chromosome 1.

To estimate the copy number of the circular form of SE-6945 in the cell population, we first searched for Illumina reads of strain LN95 that spanned *attS* or the "hypothetical" *attB*. Although next-generation sequencing reads were obtained at 229× chromosome coverage, no reads spanning *attS* or *attB* were detected [44]. Quantitative PCR further revealed that the mean *attS* to *gyrB* ratio was 0.0012 (S8 Fig B). This relative copy number was consistent with the result from a previous study detecting the circular form of SE-6283 in *E. coli*, which showed an *attS* to chromosome ratio of 0.001 [30].

To determine the nicking site on *attL* and *attR* (Fig 5 C), we cloned the PCR products of *attS* and then sequenced ten cloned molecules. Based on the *attL*, *attR*, and the original *attB* sequences in the TJ249 chromosome (S3 Fig, S4 Fig), we hypothesized four nicking sites

(arrowheads in Fig 5 C) in *attL* and *attR* on pSEA2 and chromosome 1 in strain 04Ya249. The cloned *attS* PCR products of 04Ya249 contained a 6 bp spacer sequence between C and C' (Fig 5 D). This observation supports the hypothesis that nicking occurs 6 bp upstream at the C end and the C' end and/or 6 bp upstream at the C' end and the C end. Two sequences, 5'-TTTTTT-3' (*attS* type 1) and 5'-TTTTCT-3' (*attS* type 2) were detected at a 1:9 ratio in the spacer region between C and C' in strain 04Ya249 (examples of the Sanger sequencing trace files have been posted in figshare [44]). These two types of spacer sequences can arise from both pSEA2 and chromosome 1 (Fig 5 D). However, only one sequence (*attS* type 1) was detected in the pSEA2-free strain LN95 (Fig 5 D), indicating that strand exchange occurs only on the top strand in *attL* × *attR* recombination on chromosome 1 (Fig 5 C). The occurrence of *attS* type 1 and *attS* type 2 in 04Ya249 (Fig 5 D) agrees with the top strand exchange in *attL* × *attR* recombinations on chromosome 1 and pSEA2, respectively (Fig 5 C). Collectively, these observations are consistent with the model that SE-6945 follows Path 1 (Fig 5 A) without undergoing strand exchange of the bottom strand in *V. alfacsensis*.

Nicking of one strand of the double stranded DNA and its circularization is often seen in the reactions mediated by HUH endonucleases (relaxase/rolling-circle replication initiator) [45]. To confirm that observed nicking at *attL* and *attR* is independent of HUH endonucleases produced from plasmids or other mobile elements in *V. alfaccensis*, the production of *attS* was additionally investigated using *E. coli* strain LN52 that carries a single copy of SE-6945 but lacks pSEA2. *attS* was produced even in LN52 (S8 Fig C). Therefore, strand-biased (top strand only) *attL* × *attR* recombination is likely mediated by DNA strand exchange enzymes encoded by SE-6945.

The insertion copy number and location of SE-6945 affects Ap resistance levels of the host cell

The naturally occurring strains 04Ya249 and 04Ya108 carry two copies of SE-6945 in their genomes. However, it remains unclear whether increased SE copies in a genome confer an advantage to the host cell. Three copies of SE-6945 in the transconjugant TJ249 were initially detected by genome sequencing. Southern hybridization analysis of other JW0452 transconjugants revealed one to two copies of SE-6945 in their genomes (S5 Fig). The location of SE-6945 became evident based on Southern hybridization for 15 among 19 transconjugants. Therefore, we used these transconjugant strains to test whether multiple integrations of SE-6945 or its integration location can increase the Ap resistance phenotype of the transconjugants.

Sixteen *E. coli* strains with or without SE-6945 were grown in Luria-Bertani broth with Ap, and then the minimum inhibitory concentrations (MICs) against individual strains were determined using the broth dilution method following the Clinical Laboratory Standards Institute (CLSI) guidelines. The MIC was highest in the clone carrying three copies of SE-6945, followed by the group of transconjugants carrying two copies and the group carrying one copy, and the MIC was the lowest in JW0452 (Fig 6). Although within-group variation was also observed, the increased copy number of SE-6945 in the genome generally resulted in the increased Ap resistance of the host cell.

The MICs of strains are shown in Table S1. There was a trend that strains with SE-6945 integrated into *insJ* showed a higher MIC than strains with integration into *yjjNt*. Thus, the location of SEs can also affect phenotype variation, possibly due to the differences in the expression levels of their cargo genes.

Fig 6. The copy number of SE-6945 affects the Ap resistance level. Sixteen transconjugants and a control strain (JW0452) were divided into four groups shown in distinct colors based on the SE-6945 copy number in the genome. MIC of ampicillin is shown according to copy number.

Discussion

Vibrio is one of the major bacterial genera found in marine sediments [46], and is among the most common microbiota of wild and farmed shrimp [47] and fish [48,49]. Several members of the genus *Vibrio* are pathogens of fishes reared in aquaculture [50], while other subsets of *Vibrio* species, including *V. cholerae*, *V. parahaemolyticus,* and *V. vulnificus*, which are ubiquitous in relatively low-salinity sea water, are human pathogens from seafood and/or water. [50,51]. Thus, *Vibrio* can be considered as a key genus aiding movement of AMR genes between aquatic environments and human-associated environments. Indeed, the accumulation of AMR genes in this genus has attracted increased research attention, particularly in *V. cholerae* [52,53]. However, direct experimental evidence for AMR gene transfer from *Vibrio* species to other human-relevant bacteria is limited.

Known genetic mechanisms of AMR gene transfer from *Vibrio* include A/C plasmids [54,55], unclassified conjugative plasmids [56], pAQU1-type MOB_H-family conjugative plasmids [57], pSEA1-type MOB_H-family conjugative plasmids [30], ICEs [58], IMEs [19], and a combination of a sedentary chromosomal integron and a conjugative plasmid carrying an integron [59]. The host range of pSEA1-type MOB_H plasmids, discovered in *V. alfacsensis* (for which only one complete genome was available until the present study), is unknown. In this

436 study, we investigated how a pSEA1-like plasmid can contribute to AMR gene transfer in a
437 laboratory setting.
438 In contrast to A/C plasmids, autonomous replication of pSEA2 and pSEA1 was
439 difficult to achieve in *E. coli,* since transconjugant selection generally yielded *E. coli* clones
440 carrying plasmid DNA integrated into the chromosome. The current most likely mechanism
441 behind this phenomenon is transposition of SE followed by homologous recombination,
442 which enabled AMR gene transfer beyond the plasmid's replication host range. This mode of
443 horizontal gene transfer may be important among marine bacteria, since the plasmid
444 conjugation host range is expected to be wider than the replication host range [60,61].
445 pSEA1 was found to carry two SEs (SE-6283 and SE-6945). However, in the previous
446 study [30], only transposition of SE-6283 was observed, likely because we did not recognize
447 SE-6945 on pSEA1 and did not intend to detect its transposition. The newly identified SE-
448 6945 is the smallest SE identified to date (Fig 2 and Fig 3), and the only known SE harboring
449 an AMR gene. As SEs can have more than one target site in a single genome, they may
450 contribute to microbial adaptation to the antimicrobials used at aquaculture sites, with
451 diverse mechanisms beyond mediating the horizontal transmission of AMR genes, such as
452 increasing the resistance level or gene redundancy preceding evolutionary innovation of an
453 AMR gene [62].
454 The discovery of SE-6945 highlights four potential core genes (*intA*, CDS2, *intB*, and
455 CDS4) present in SEs. However, the specific roles of these gene products in their
456 transposition steps remain to be determined. Among the types of transposon movement
457 classified by Curcio and Derbyshire [15], 'copy-out' is currently the most consistent with our
458 observations of SEs regarding the first step of its location change. One model for strand
459 exchange on single stranded DNA mediated by tyrosine recombinase, leading to a single

stranded circle, has been proposed for integron gene cassette excision (replicative resolution model in [43]). In the replicative resolution model, strand exchange between two folded *attC* bottom strands and the following replication generates a gene cassette circle with *attC* and results in the removal of one gene cassette with *attC* from the gene cassette array on the donor molecule. This can cause formation of integron variants with fewer gene cassettes and even integrons with an empty *attI,* as observed in *in vivo* experiments [42]. SE circle formation rarely leaves the empty *attB* (Fig 5 B (i) and [30]). Thus the rejoining of the host DNA side at nicking sites is somehow prevented, possibly by the action of multiple proteins involved: possibly the CDS2, CDS4 products, unlike the movement of gene cassettes. Currently, we do not have information on the fate of the nicked donor molecule. Unlike DDE transposases, tyrosine recombinases usually do not generate a free 3′ OH end and are covalently linked to the phosphate of substrate DNA (Fig 5 A) [63]. Therefore, a process equivalent to DPC repair [40], which might require both host and SE-encoding factors, is necessary to achieve the IS*3*-like copy-out process. Nonetheless, we speculate that the alternate single stranded DNA circle generation route, accompanying chromosome loss (bottom left in Fig 5 A), is a less likely route as it does not give any advantage to target site-selective and putatively non-transferrable SEs left in dying cells.

While strand-biased *attL* × *attR* recombination was repeatedly observed for the two SEs, not much information has been obtained regarding their integration~~ step~~. While 6 bp from the 5′ end of C at *attL* on the donor molecule is incorporated into a circular SE copy, the incorporated 6 bp tends to be placed next to the 3′ end of C′ at *attR* after integration into the target site (see *attL* on pSEA2 and *attRs* on TJ249, and previously detected SE-6283 in transposition from pSEA1 to *bcp* in *E. coli*). Thus, there seems to be a strict rule in the order of strand exchange at the integration step, but determining the precise order of

484 nicking and nicking sites on the two strands during the integration step requires further
485 investigations.
486 A notable difference between IS and SE is the strong strand bias unique to SE upon
487 strand exchange: some ISs can generate a single stranded bridge using either of the two
488 strands (but not both simultaneously) [64,65], while SEs use only top strand. The
489 dissimilarity between SE and ICE/IMEs is that ICE/IMEs encode the recombination
490 directionality factor Xis [25], while SEs do not encode Xis homologs. CDS2 or CDS4 products
491 may function exclusively in either the initial circularization step or the integration as the
492 recombination directionality factor. Another dissimilarity between SE and ICE/IME is that
493 the former does not encode an HUH endonuclease. There is still a possibility that SEs carry
494 an *oriT* recognized by a family of relaxases and are mobilized like CIME [21], though we
495 could not identify an *oriT* in SE-6945 or SE-6283 by local similarity search alone. It may also
496 be possible that IntB, a large tyrosine recombinase, functions as a relaxase, since a
497 conjugative plasmid from *Clostridium* has been shown to use a tyrosine recombinase
498 homolog as a conjugative relaxase [66].
499 We propose that interplay between SEs and conjugative MDR plasmids contribute to
500 AMR gene transmission in marine bacteria. Further biochemical and bioinformatic studies
501 on SEs are needed to reveal the mechanisms of gene transfer among the genus *Vibrio* and
502 other aquaculture-associated bacteria.
503 To refer to transposable individual SE members, we used numbers that are
504 compatible with the existing transposon database [33]. However, further debate is needed
505 regarding handling SEs in mobile DNA databases.
506

Materials and methods

Strains, plasmids, and culture media

Strains and plasmids used in the study are listed in Table 1. Strain 04Ya108 was previously identified as *Vibrio ponticus* based on 16S rRNA gene sequence similarity. However, determination of the complete sequence in this study revealed that it shows >96% average nucleotide identity to *V. alfacsensis* strain CAIM 1831 (DSM 24595) (S1 Fig B) [67]. Therefore, strain 04Ya108 was re-classified as *V. alfacsensis*. Strain LN95 is a pSEA2-free tetracycline-susceptible derivative of strain 04Ya249. This strain was generated through a repeated batch culture of 04Ya249, and subsequent single-colony isolation. The absence of pSEA2 from LN95 was confirmed by next-generation sequencing.

Table 1. Strains and plasmids used.

Strains or plasmids	Relevant genotype, phenotype, descriptions[a]	Reference
Vibrio alfacsensis		
04Ya249	Aquaculture isolate harboring conjugative plasmid pSEA2; Tc^r, Ap^r, Ery^r Cm^r	[27]
04Ya108	Aquaculture isolate harboring conjugative plasmid pSEA1; Tc^r, Ap^r, Ery^r Cm^r	[27]
LN95	pSEA2 free derivative of strain 04Ya249; Ap^r	This study
E. coli		
DH5α	F^-, Φ80d*lacZ*ΔM15, Δ(*lacZYA-argF*)U169, *deoR*, *recA*1, *endA*1, *hsdR*17(r_K^-, m_K^+), *phoA*, *supE*44, λ^-, *thi*-1, *gyrA*96, *relA*1	Takara Bio Inc., Shiga, Japan
JW0452	λ- *rph-1* Δ(*rhaD-rhaB*)*568 hsdR514* Δ*lacZ4787*(::*rrnB-3*) Δ*(araD-araB)567* Δ*acrA748*::*kan*; Km^r	[68]
JW0452rif	Spontaneous rifampicin-resistant mutant of JW0452	This study
JW0452Δ *recA*	JW0452Δ*recA::cat*; Km^r, Cm^r	This study
JW0452Δ *recA*rif	Spontaneous rif resistant mutant of JW0452Δ*recA*; Km^r, Cm^r, Rif^r	This study

Transconjugants[c]		
TJ249	JW0452 *insJ*::SE-6945::pSEA2 *yjjNt*::SE-6945; Ap^r Tc^r Ery^r Cm^r	This study
LN28, LN32, LN36, LN86	JW0452 chr::pSEA2[b]; Ap^r Tc^r Ery^r Cm^r	This study
LN29, LN30, LN82, LN88, LN91	JW0452 *yjjNt*::SE-6945::pSEA2; Ap^r Tc^r Ery^r Cm^r	This study
LN33, LN34, LN35, LN37, LN58, LN84, LN89, LN90	JW0452 *insJ:*::SE-6945::pSEA2; Ap^r Tc^r Ery^r Cm^r	This study
LN52	JW0452 *yjjNt*::SE-6945; Ap^r	This study
LN52rif	Spontaneous rifampicin-resistant mutant of LN52; Rif^r, Ap^r	This study
Plasmids		
pGEM-T	Cloning vector; pUC replicon, Ap^r	Promega, Madison, WI, USA
pGEM-attS	pGEM-T carrying the 206 bp *attS* fragment; pUC replicon, Ap^r	This study
pGEM-int	pGEM-T carrying the 103 bp *intA* fragment; pUC replicon, Ap^r	This study
pGEM-gyrB	pGEM-T carrying the 110 bp *gyrB* fragment from strain 04Ya249; pUC replicon, Ap^r	This study
pKD46	Lambda-Red recombinase expression plasmid; pSC101ts replicon, Ap^r	[69]
pKD3	Donor of the *cat* gene for the Lambda-Red recombination experiment; R6K replicon, Cm^r	[69]

a. Antimicrobial resistance phenotypes (^{r}) listed were confirmed by experiments. Abbreviations are as follows: Ap, ampicillin; Tc, tetracycline: Ery, erythromycin; Cm, chloramphenicol; Rif, rifampicin; *kan*, kanamycin resistance gene. *yjjNt* denotes the putative transcription termination region for the *yjjN* gene. It is unclear whether the resistance genes on pSEA2 are still in the original locations for other transconjugants besides TJ249.

b. Cointegration of plasmid pSEA2 with chromosome, independent of SE-6945 transposition. Location of pSEA2 in the transconjugant genome could not be defined based on Southern hybridization results.

527 *c.* The 19 transconjugants listed (TJ249, LN28, LN29, LN30, LN32, LN33, LN34, LN35, LN36,
528 LN37, LN52, LN58, LN82, LN84, LN86, LN88, LN89, LN90, LN91) were obtained from 19
529 independent mating experiments. Selection was done at 42 °C. Antibiotic selection used was
530 as follows: Tc for LN28, LN29 LN30, LN32, LN33, LN34, LN35, LN36, and LN37; Ap for LN52;
531 Ap Tc for LN58 LN82, LN84, LN86, LN88, LN89, LN90, and LN91; Ery for TJ249.
532
533 The presence of a single SE-6945 copy in the LN52 genome was confirmed by
534 Southern hybridization (S5 Fig). The *recA*-null mutant of JW0452, JW0452Δ*recA*, was
535 constructed using the lambda-Red method [69]. A DNA fragment containing the 5′ and 3′
536 sequences of the *recA* gene and a chloramphenicol resistance gene was amplified by PCR
537 using primers YO-175 and RecA_stop_primingsite_2 (Table 2) and plasmid pKD3 [69] as a
538 template. The PCR products (700 ng) were introduced into electrocompetent cells of
539 JW0452 carrying pKD46 by electroporation using a Gene Pulser Xcell™ (BioRad, Hercules,
540 CA, USA). The occurrence of recombination at the expected site was confirmed by PCR using
541 primers CAT-584 and BW25113_2815723f (Table 2). The absence of the *recA* gene was also
542 confirmed by PCR using primers LN192_recA1 and LN193_recA2.
543 *Vibrio alfacsensis* strains were cultured in BD Bacto™ brain heart infusion medium
544 (BD237500; Becton, Dickinson, and Company, Franklin Lakes, NJ, USA) supplemented with
545 up to 2% NaCl at 25 °C. *E. coli* strains were cultured in BD Difco™ LB Broth, Miller
546 (BD244520; Becton, Dickinson, and Company) at 37 °C or 42 °C. BD Difco™ Mueller Hinton
547 Broth (BD 275730; Becton, Dickinson, and Company) was used for antibiotic susceptibility
548 testing of *E. coli*. BD Difco™ Marine Broth 2216 (BD279110; Becton, Dickinson, and
549 Company) was used for filter mating. Solid media were prepared by adding 1.5% agar to the
550 broth. Antibiotics were added to the medium at the following concentrations when

551 required: erythromycin (Nacalai Tesque, Kyoto, Japan), 100 μg/ml; tetracycline (Nacalai

552 Tesque), 10 μg/ml; rifampicin (Sigma-Aldrich, St. Louis, MO, USA), 50 μg/ml; ampicillin

553 (Nacalai Tesque), 100 μg/ml.

554

555 **Table 2. Oligonucleotides used.**

Name	Sequence (5' to 3')	Purpose
LN112	GGGTTACCTTCCCAATGCGT	Southern hybridization probe for SE-6945 *intA*
LN113	CGACTGTTGGTAGCGACTGT	Southern hybridization probe for SE-6945 *intA*
LN_142_junction2	AAGATGGTAAAAGTGTTCCA	Detection of *attS* (206 bp) by qPCR and *attL* (304 bp) by standard PCR
LN_143_junction2	TTTGTGTGTAGCCCTTGTG	Detection of *attS* (206 bp) by qPCR and *attR* (248 bp) by standard PCR
LN_150_intA2	GGTTATGTGGAGAAGTTGCC	Detection of *intA* (103 bp) by qPCR
LN_151_intA2	TGAGTTCGGTTTCTTGCTTC	Detection of *intA* (103 bp) by qPCR
LN_181_attB_L	CGAGGGTAAAGTGCCAACAT	Detection of chromosomal *attB* (345 bp if empty, 7.4 kb if occupied) and *attL* (304 bp) by standard PCR (04Ya249)

LN183_attB_R2	ACATCAGCAGGAGTTAGTTG	Detection of chromosomal *attB* (345 bp, 7.4 kb) and *attR* (248 bp) by standard PCR (04Ya249)
LN184_gyrBf1	AACAGAATTGCACCCAGAAG	Detection of *gyrB* (110 bp) by qPCR (04Ya249)
LN185_gyrBr1	GAAGACCGCCTGATACTTTG	Detection of *gyrB* (110 bp) by qPCR (04Ya249)
YO-175	CAGAACATATTGACTATCCGGTATTACCCGGCATGACAGGAGTAAAAATGTGTAGGCTGGAGCTGCTTCG	Amplification of *cat* gene for Lambda-Red recombination
RecA_stop_primingsite_2	ATGCGACCCTTGTGTATCAAACAAGACGATTAAAAATCTTCGTTAGTTTCCATATGAATATCCTCCTTA	Amplification of *cat* gene for Lambda-Red recombination
CAT-584	AAGCCATCACAAACGGCATG	Confirmation of *cat* gene insertion
BW25113_2815723f	AATACGCGCAGGTCCATAAC	Confirmation of *cat* gene insertion
LN192_recA1	GTTCCATGGATGTGGAAACC	Confirmation of *recA* deletion
LN193_recA2	ATATCGACGCCCAGTTTACG	Confirmation of *recA* deletion

556

557 ## Conjugation

558 The donor *Vibrio* strain and *E. coli* recipient strains were grown overnight at 25 °C and 37 °C,
559 respectively. A 500 μl aliquot of each culture was mixed, centrifuged, and resuspended in 50
560 μl of Luria-Bertani broth. The cell mixture was spotted on a 0.45 μm pore-size nitrocellulose
561 filter (Merck, Millipore Ltd., Tullagreen, Ireland) placed on marine broth agar, and allowed
562 to mate for 24 h at 25 °C. After incubation, the cell mixture on the filter was serially diluted
563 in 1× phosphate-buffered saline, and then 100 μl of the mixture was plated on an
564 appropriate agar medium to measure the CFU and incubated at 42 °C to suppress growth of
565 *Vibrio* strains. After genome sequence determination of TJ249, more than 17 independent
566 mating experiments were performed to obtain insights into the variation of pSEA2
567 integration patterns using JW0452 as the recipient, and transconjugants were screened at
568 42 °C in the presence of Tc alone, Ap alone, or both Ap and Tc. The AMR phenotype of each
569 transconjugant was further determined after single-colony isolation using Ery, Cm, Ap, and
570 Tc (Table 1).

571 Quantitative mating assays (Fig 4) were performed to address the involvement of
572 homologous recombination in pSEA2 integration using strains JW0452rif, JW0452Δ*recA*rif,
573 and LN95rif as recipients. Selection conditions for transconjugants were Rif Ap Tc 42 °C or
574 Rif Ap 42 °C. The *Vibrio* donor strain was selected on brain heart infusion agar with 2% NaCl
575 supplemented with Tc at 25 °C. CFUs of donor, recipient, and transconjugant were
576 determined after 24 hours of incubation.

577

578 ## PCR experiments

579 The PCR detection of *attL*, *attR,* and *attS* was performed using TaKaRa Ex Taq (TaKaRa Bio
580 Inc., Kusatsu, Japan), and genomic DNA of 04Ya249, LN95, and LN52 prepared using QIAGEN
581 DNeasy Blood & Tissue kit (QIAGEN GmbH, Hilden, Germany). PCR premix was prepared in a
582 50 μl scale, and 1 μl of the template (10 ng/μl) was added to the reaction mix throughout
583 the study. The PCR cycle used was 94 °C for 1 min, followed by 35 cycles of 94 °C for 30 s
584 and 60 °C for 30 s. As the empty *attB* was not amplified using TaKaRa Ex Taq, we conducted
585 additional long PCR using LA Taq polymerase (TaKaRa Bio Inc.) to detect occupied *attB* and
586 confirm the functionality of primers used for detection of empty *attB*. The PCR cycles used
587 for long PCR were 1 cycle of 94 °C for 1 min, followed by 35 cycles of 95 °C for 1 min, 65 °C
588 for 1 min, and 72 °C for 1 min. PCR products of *attS* were further cloned using the pGEM-T
589 easy vector system (Promega, Madison, WI, USA) and DH5α competent cells to analyze the
590 sequence variation of PCR products.

591 Quantitative PCR was performed using THUNDERBIRD® SYBR qPCR Mix (Toyobo,
592 Osaka, Japan) and a CFX connect Real-Time system (BioRad, Hercules, CA, USA) and a two-
593 step PCR protocol of 40 cycles of 95 °C for 5 s and 60 °C for 30 s. Target quantity was
594 estimated based on a standard curve of the control plasmid DNA (pGEM-*gyrB*, pGEM-*intA*,
595 pGEM-*attS*) constructed by TA cloning. Primers used and their purposes are listed in Table 2
596 and Fig 5 legend.

597

598 ## Southern hybridization

599 The copy number and integration location of SE-6945 in transconjugants (JW0452
600 derivatives) were analyzed by Southern hybridization using the 5' end of *intA*, amplified

601 using primers LN112 and LN113 (Table 2) and the PCR DIG Synthesis Kit (Roche, Basel,
602 Switzerland) as a probe. Genomic DNA (2.5 μg) was double digested with either *Nde*I and
603 *Sph*I or *Nde*I and *Hin*dIII (New England Biolabs, Ipswich, MA, USA), then electrophoresed in
604 0.8% agarose gel. Separated DNA fragments were transferred to the nitrocellulose
605 membranes (Amersham Hybond-N+; GE Healthcare UK Ltd., Buckinghamshire, UK) by
606 capillary transfer. The probe was detected using CDT-star® (Roche). Restriction map for the
607 DNA segments around SE-6945 integration locations and the expected size of DNA segments
608 with probe signal are shown in S5 Fig A.
609

610 ## Antimicrobial susceptibility testing

611 To examine the antimicrobial susceptibility of transconjugants harboring one to three SE-
612 6945 copies, the MIC of ampicillin was determined using the broth dilution method in 96-
613 well microtiter plate format according to standard M07 of the CLSI [70]. The Ap
614 concentrations tested were 1000, 500, 250, 125, 62.5, 31.25, 16, 8, 4, and 2 μg/ml. The test
615 plates were incubated at 35 °C for 24 h.
616

617 ## Genome sequencing

618 Genomic DNA was extracted from 250–500 μl of *V. alfacsensis* strains 04Ya249, 04Ya108, or
619 *E. coli* strain TJ249 culture using the QIAGEN DNeasy Blood & Tissue kit (QIAGEN GmbH).
620 The extracted genomic DNA was sequenced on the PacBio RS II platform using P6C4
621 chemistry at Macrogen (Tokyo, Japan) in 2016. Genome assembly was conducted using
622 HGAP v.3 [71] for *Vibrio* strains and Flye v 2.8.3-b1695 for *E. coli* TJ249 [72]. Reads were
623 obtained at >120× coverage for the chromosomes of each strain. Reads and the genome

sequence of TJ249 have been posted to figshare [73]. Illumina reads of the pSEA2-free strain LN95 were obtained using the TruSeq PCR-free library and NovaSeq 6000 platform at NovogeneAIT Genomics Singapore Pte., Ltd. (Singapore) to confirm the loss of pSEA2 and to identify the circular form of SE-6945. The mapping results have been posted to figshare [44]. Genomes were compared using MUMmer3.23 [74] and GenomeMatcher [75]. AMR genes in the assembly were searched for using AMRFinderPlus [76]. The average nucleotide identity was determined using fastANI [77].

Searches for SE-6945 and SE-6283-related SEs

Nucleotide sequences of the SE core gene region (*intA*, CDS2, *intB*, CDS4) (6432 bp for SE-6283, 5541 bp for SE-6945) were used as queries in blastn searches against the NCBI nucleotide collection (nr/nt) database (August 3, 2021). Hit subjects showing > 85 % nucleotide identity with > 99% query coverage were regarded as close relatives of SE-6945 or SE-6283, and were further investigated as to their integration locations.

Data availability

Sequence data generated in this study and their availability are summarized in Table S2. The complete genome sequences of strains 04Ya108 and 04Ya249 were submitted to GenBank/DDBJ/EMBL under accession numbers AP024165 (chr1 of 04Ya108), AP024166 (chr2 of 04Ya108), AP024167 (pSEA1 of 04Ya108), AP024168 (pYa108 of 04Ya108), AP019849 (chr1 of 04Ya249), AP019850 (chr2 of 04Ya249), AP019851 (pSEA2 of 04Ya249), and AP019852 (pVA249 of 04Ya249). The raw reads for strains 04Ya108, 04Ya249, LN95 and

TJ249 are available from Sequence Read Archive under accession numbers DRA011098, DRA008632, DRA011762, and DRA013462, respectively.

Acknowledgments

We thank the National Bioresource Project of the National Institute of Genetics, Japan, for providing the *E. coli* strains BW25113, JW2669, and JW0452. We thank Atsushi Ota and Fumito Maruyama at Hiroshima University for their support for the annotation on the TJ249 assembly. We thank Yuichi Otsuka at Saitama University for helpful discussions and Yuta Sugimoto at Ehime University for experimental support. We thank Kenji K Kojima at Genetic Information Research Institute for the discussion on transposon classification, and Yasukazu Daigaku at Tohoku University for the discussion on DNA protein cross link repair. We thank Editage for language editing (job number LINON_4_4).

References

1. Cabello FC, Godfrey HP, Tomova A, Ivanova L, Dölz H, Millanao A et al. (2013) Antimicrobial use in aquaculture re-examined: its relevance to antimicrobial resistance and to animal and human health. Environ Microbiol 15: 1917-1942.
2. Cabello FC, Godfrey HP, Buschmann AH, Dölz HJ (2016) Aquaculture as yet another environmental gateway to the development and globalisation of antimicrobial resistance. Lancet Infect Dis 16: e127-e133.
3. Magiorakos AP, Srinivasan A, Carey RB, Carmeli Y, Falagas ME, Giske CG et al. (2012) Multidrug-resistant, extensively drug-resistant and pandrug-resistant bacteria: an

international expert proposal for interim standard definitions for acquired resistance. Clin Microbiol Infect 18: 268-281.

4. Karakonstantis S, Kritsotakis EI, Gikas A (2020) Pandrug-resistant Gram-negative bacteria: a systematic review of current epidemiology, prognosis and treatment options. J Antimicrob Chemother 75: 271-282.

5. Rodríguez-Beltrán J, DelaFuente J, León-Sampedro R, MacLean RC, San Millán Á (2021) Beyond horizontal gene transfer: the role of plasmids in bacterial evolution. Nat Rev Microbiol 19: 347-359.

6. Johnson CM, Grossman AD (2015) Integrative and Conjugative Elements (ICEs): What They Do and How They Work. Annu Rev Genet 49: 577-601.

7. Yano H, Rogers LM, Knox MG, Heuer H, Smalla K, Brown CJ et al. (2013) Host range diversification within the IncP-1 plasmid group. Microbiology (Reading) 159: 2303-2315.

8. Dahmane N, Libante V, Charron-Bourgoin F, Guédon E, Guédon G, Leblond-Bourget N et al. (2017) Diversity of integrative and conjugative elements of *Streptococcus salivarius* and their intra- and interspecies Transfer. Appl Environ Microbiol 83: e00337-17.

9. Cabezón E, Lanka E, de la Cruz F (1994) Requirements for mobilization of plasmids RSF1010 and ColE1 by the IncW plasmid R388: *trwB* and RP4 *traG* are interchangeable. J Bacteriol 176: 4455-4458.

10. Carraro N, Matteau D, Luo P, Rodrigue S, Burrus V (2014) The master activator of IncA/C conjugative plasmids stimulates genomic islands and multidrug resistance dissemination. PLoS Genet 10: e1004714.

691 11. Daccord A, Ceccarelli D, Burrus V (2010) Integrating conjugative elements of the
692 SXT/R391 family trigger the excision and drive the mobilization of a new class of *Vibrio*
693 genomic islands. Mol Microbiol 78: 576-588.
694 12. Garcillán-Barcia MP, Francia MV, de la Cruz F (2009) The diversity of conjugative
695 relaxases and its application in plasmid classification. FEMS Microbiol Rev 33: 657-687.
696 13. Villa L, Carattoli A (2020) Plasmid typing and classification. Methods Mol Biol 2075:
697 309-321.
698 14. Roberts AP, Chandler M, Courvalin P, Guédon G, Mullany P, Pembroke T et al. (2008)
699 Revised nomenclature for transposable genetic elements. Plasmid 60: 167-173.
700 15. Curcio MJ, Derbyshire KM (2003) The outs and ins of transposition: from mu to
701 kangaroo. Nat Rev Mol Cell Biol 4: 865-877.
702 16. Bouvier M, Demarre G, Mazel D (2005) Integron cassette insertion: a recombination
703 process involving a folded single strand substrate. EMBO J 24: 4356-4367.
704 17. Val ME, Bouvier M, Campos J, Sherratt D, Cornet F, Mazel D et al. (2005) The single-
705 stranded genome of phage CTX is the form used for integration into the genome of
706 Vibrio cholerae. Mol Cell 19: 559-566.
707 18. Doublet B, Boyd D, Mulvey MR, Cloeckaert A (2005) The *Salmonella* genomic island 1 is
708 an integrative mobilizable element. Mol Microbiol 55: 1911-1924.
709 19. Carraro N, Rivard N, Ceccarelli D, Colwell RR, Burrus V (2016) IncA/C conjugative
710 plasmids mobilize a new family of multidrug resistance islands in clinical *Vibrio*
711 *cholerae* non-O1/non-O139 isolates from Haiti. mBio 7: e00509-16.
712 20. Pavlovic G, Burrus V, Gintz B, Decaris B, Guédon G (2004) Evolution of genomic islands
713 by deletion and tandem accretion by site-specific recombination: ICE*St1*-related
714 elements from *Streptococcus thermophilus*. Microbiology (Reading) 150: 759-774.

715 21. Achard A, Leclercq R (2007) Characterization of a small mobilizable transposon,
716 MTn*Sag1*, in *Streptococcus agalactiae*. J Bacteriol 189: 4328-4331.
717 22. Guédon G, Libante V, Coluzzi C, Payot S, Leblond-Bourget N (2017) The obscure world
718 of integrative and mobilizable elements, highly widespread elements that pirate
719 bacterial conjugative systems. Genes (Basel) 8: E337.
720 23. Caparon MG, Scott JR (1989) Excision and insertion of the conjugative transposon
721 Tn*916* involves a novel recombination mechanism. Cell 59: 1027-1034.
722 24. Auchtung JM, Lee CA, Monson RE, Lehman AP, Grossman AD (2005) Regulation of a
723 *Bacillus subtilis* mobile genetic element by intercellular signaling and the global DNA
724 damage response. Proc Natl Acad Sci U S A 102: 12554-12559.
725 25. Burrus V, Waldor MK (2003) Control of SXT integration and excision. J Bacteriol 185:
726 5045-5054.
727 26. Naito M, Ogura Y, Itoh T, Shoji M, Okamoto M, Hayashi T et al. (2016) The complete
728 genome sequencing of *Prevotella intermedia* strain OMA14 and a subsequent fine-
729 scale, intra-species genomic comparison reveal an unusual amplification of conjugative
730 and mobile transposons and identify a novel *Prevotella*-lineage-specific repeat. DNA
731 Res 23: 11-19.
732 27. Nonaka L, Ikeno K, Suzuki S (2007) Distribution of tetracycline resistance gene, *tet(M)*,
733 in Gram-positive and Gram-negative bacteria isolated from sediment and seawater at
734 a coastal aquaculture site in Japan. Microbes Environ 22: 355-364.
735 28. Nonaka L, Maruyama F, Miyamoto M, Miyakoshi M, Kurokawa K, Masuda M (2012)
736 Novel conjugative transferable multiple drug resistance plasmid pAQU1 from
737 *Photobacterium damselae* subsp. *damselae* isolated from marine aquaculture
738 environment. Microbes Environ 27: 263-272.

29. Nonaka L, Maruyama F, Suzuki S, Masuda M (2015) Novel macrolide-resistance genes, *mef*(C) and *mph*(G), carried by plasmids from *Vibrio* and *Photobacterium* isolated from sediment and seawater of a coastal aquaculture site. Lett Appl Microbiol 61: 1-6.

30. Nonaka L, Yamamoto T, Maruyama F, Hirose Y, Onishi Y, Kobayashi T et al. (2018) Interplay of a non-conjugative integrative element and a conjugative plasmid in the spread of antibiotic resistance via suicidal plasmid transfer from an aquaculture *Vibrio* isolate. PLoS One 13: e0198613.

31. Neela FA, Nonaka L, Suzuki S (2007) The diversity of multi-drug resistance profiles in tetracycline-resistant *Vibrio* species isolated from coastal sediments and seawater. J Microbiol 45: 64-68.

32. Alcock BP, Raphenya AR, Lau TTY, Tsang KK, Bouchard M, Edalatmand A et al. (2020) CARD 2020: antibiotic resistome surveillance with the comprehensive antibiotic resistance database. Nucleic Acids Res 48: D517-D525.

33. Tansirichaiya S, Rahman MA, Roberts AP (2019) The transposon registry. Mob DNA 10: 40.

34. Pei J, Kim BH, Grishin NV (2008) PROMALS3D: a tool for multiple protein sequence and structure alignments. Nucleic Acids Res 36: 2295-2300.

35. Nunes-Düby SE, Kwon HJ, Tirumalai RS, Ellenberger T, Landy A (1998) Similarities and differences among 105 members of the Int family of site-specific recombinases. Nucleic Acids Res 26: 391-406.

36. Landy A (1989) Dynamic, structural, and regulatory aspects of lambda site-specific recombination. Annu Rev Biochem 58: 913-949.

37. Schneider TD, Stephens RM (1990) Sequence logos: a new way to display consensus sequences. Nucleic Acids Res 18: 6097-6100.

763 38. Stokes HW, O'Gorman DB, Recchia GD, Parsekhian M, Hall RM (1997) Structure and
764 function of 59-base element recombination sites associated with mobile gene
765 cassettes. Mol Microbiol 26: 731-745.
766 39. Stokes HW, Hall RM (1989) A novel family of potentially mobile DNA elements
767 encoding site-specific gene-integration functions: integrons. Mol Microbiol 3: 1669-
768 1683.
769 40. Zhang H, Xiong Y, Chen J (2020) DNA-protein cross-link repair: what do we know now.
770 Cell Biosci 10: 3.
771 41. Chandler M, Fayet O, Rousseau P, Ton Hoang B, Duval-Valentin G (2015) Copy-out-
772 paste-in transposition of IS*911*: a major transposition pathway. Microbiol Spectr 3:
773 42. Collis CM, Hall RM (1992) Site-specific deletion and rearrangement of integron insert
774 genes catalyzed by the integron DNA integrase. J Bacteriol 174: 1574-1585.
775 43. Escudero JA, Loot C, Nivina A, Mazel D (2015) The integron: adaptation on demand.
776 Microbiol Spectr 3: MDNA3-0019.
777 44. Yano H, Nonaka L (2021) Illumina reads analysis of *Vibrio alfacsensis* pSEA2-free strain
778 LN95. URL: https://doiorg/106084/m9figshare14338883
779 45. Chandler M, de la Cruz F, Dyda F, Hickman AB, Moncalian G, Ton-Hoang B (2013)
780 Breaking and joining single-stranded DNA: the HUH endonuclease superfamily. Nat
781 Rev Microbiol 11: 525-538.
782 46. Chen J, McIlroy SE, Archana A, Baker DM, Panagiotou G (2019) A pollution gradient
783 contributes to the taxonomic, functional, and resistome diversity of microbial
784 communities in marine sediments. Microbiome 7: 104.
785 47. Cornejo-Granados F, Lopez-Zavala AA, Gallardo-Becerra L, Mendoza-Vargas A, Sánchez
786 F, Vichido R et al. (2017) Microbiome of Pacific Whiteleg shrimp reveals differential

bacterial community composition between Wild, Aquacultured and AHPND/EMS outbreak conditions. Sci Rep 7: 11783.

48. Llewellyn MS, McGinnity P, Dionne M, Letourneau J, Thonier F, Carvalho GR et al. (2016) The biogeography of the atlantic salmon (*Salmo salar*) gut microbiome. ISME J 10: 1280-1284.

49. Egerton S, Culloty S, Whooley J, Stanton C, Ross RP (2018) The gut microbiota of marine fish. Front Microbiol 9: 873.

50. Thompson FL, Iida T, Swings J (2004) Biodiversity of Vibrios. Microbiol Mol Biol Rev 68: 403-431.

51. Takemura AF, Chien DM, Polz MF (2014) Associations and dynamics of *Vibrionaceae* in the environment, from the genus to the population level. Front Microbiol 5: 38.

52. Verma J, Bag S, Saha B, Kumar P, Ghosh TS, Dayal M et al. (2019) Genomic plasticity associated with antimicrobial resistance in *Vibrio cholerae*. Proc Natl Acad Sci U S A 116: 6226-6231.

53. Osei Sekyere J, Reta MA (2020) Genomic and resistance epidemiology of Gram-negative bacteria in Africa: a systematic review and phylogenomic analyses from a one health perspective. mSystems 5: e00897-20.

54. Carraro N, Sauvé M, Matteau D, Lauzon G, Rodrigue S, Burrus V (2014) Development of pVCR94ΔX from *Vibrio cholerae*, a prototype for studying multidrug resistant IncA/C conjugative plasmids. Front Microbiol 5: 44.

55. Folster JP, Katz L, McCullough A, Parsons MB, Knipe K, Sammons SA et al. (2014) Multidrug-resistant IncA/C plasmid in *Vibrio cholerae* from Haiti. Emerg Infect Dis 20: 1951-1953.

810 56. Liu M, Wong MH, Chen S (2013) Molecular characterisation of a multidrug resistance
811 conjugative plasmid from *Vibrio parahaemolyticus*. Int J Antimicrob Agents 42: 575-
812 579.
813 57. Nonaka L, Maruyama F, Onishi Y, Kobayashi T, Ogura Y, Hayashi T et al. (2014) Various
814 pAQU plasmids possibly contribute to disseminate tetracycline resistance gene *tet*(M)
815 among marine bacterial community. Front Microbiol 5: 152.
816 58. Beaber JW, Burrus V, Hochhut B, Waldor MK (2002) Comparison of SXT and R391, two
817 conjugative integrating elements: definition of a genetic backbone for the mobilization
818 of resistance determinants. Cell Mol Life Sci 59: 2065-2070.
819 59. Rowe-Magnus DA, Guerout AM, Mazel D (2002) Bacterial resistance evolution by
820 recruitment of super-integron gene cassettes. Mol Microbiol 43: 1657-1669.
821 60. Encinas D, Garcillán-Barcia MP, Santos-Merino M, Delaye L, Moya A, de la Cruz F
822 (2014) Plasmid conjugation from proteobacteria as evidence for the origin of
823 xenologous genes in cyanobacteria. J Bacteriol 196: 1551-1559.
824 61. Kishida K, Inoue K, Ohtsubo Y, Nagata Y, Tsuda M (2017) Host range of the conjugative
825 transfer system of IncP-9 naphthalene-catabolic plasmid NAH7 and characterization of
826 its *oriT* region and relaxase. Appl Environ Microbiol 83: e02359-16.
827 62. Elliott KT, Cuff LE, Neidle EL (2013) Copy number change: evolving views on gene
828 amplification. Future Microbiol 8: 887-899.
829 63. Jayaram M, Ma CH, Kachroo AH, Rowley PA, Guga P, Fan HF et al. (2015) An overview
830 of tyrosine site-specific recombination: from an Flp perspective. Microbiol Spectr 3:
831 64. Polard P, Chandler M (1995) An in vivo transposase-catalyzed single-stranded DNA
832 circularization reaction. Genes Dev 9: 2846-2858.

65. Rousseau P, Loot C, Turlan C, Nolivos S, Chandler M (2008) Bias between the left and right inverted repeats during IS911 targeted insertion. J Bacteriol 190: 6111-6118.

66. Wisniewski JA, Traore DA, Bannam TL, Lyras D, Whisstock JC, Rood JI (2016) TcpM: a novel relaxase that mediates transfer of large conjugative plasmids from *Clostridium perfringens*. Mol Microbiol 99: 884-896.

67. Gomez-Gil B, Roque A, Chimetto L, Moreira APB, Lang E, Thompson FL (2012) *Vibrio alfacsensis* sp. nov., isolated from marine organisms. Int J Syst Evol Microbiol 62: 2955-2961.

68. Baba T, Ara T, Hasegawa M, Takai Y, Okumura Y, Baba M et al. (2006) Construction of *Escherichia coli* K-12 in-frame, single-gene knockout mutants: the Keio collection. Mol Syst Biol 2: 2006.0008.

69. Datsenko KA, Wanner BL (2000) One-step inactivation of chromosomal genes in *Escherichia coli* K-12 using PCR products. Proc Natl Acad Sci U S A 97: 6640-6645.

70. Wayne PA (2018) Methods for dilution antimicrobial susceptibility tests for bacteria that grow aerobically. 11th ed. CLSI standard M07. Clinical and Laboratory Standards Institute.

71. Chin CS, Alexander DH, Marks P, Klammer AA, Drake J, Heiner C et al. (2013) Nonhybrid, finished microbial genome assemblies from long-read SMRT sequencing data. Nat Methods 10: 563-569.

72. Kolmogorov M, Yuan J, Lin Y, Pevzner PA (2019) Assembly of long, error-prone reads using repeat graphs. Nat Biotechnol 37: 540-546.

73. Yano H, Nonaka L (2021) Complete genome of transconjugant TJ249. URL: https://doiorg/106084/m9figshare13332467

74. Kurtz S, Phillippy A, Delcher AL, Smoot M, Shumway M, Antonescu C et al. (2004) Versatile and open software for comparing large genomes. Genome Biol 5: R12.

75. Ohtsubo Y, Ikeda-Ohtsubo W, Nagata Y, Tsuda M (2008) GenomeMatcher: a graphical user interface for DNA sequence comparison. BMC Bioinformatics 9: 376.

76. Feldgarden M, Brover V, Haft DH, Prasad AB, Slotta DJ, Tolstoy I et al. (2019) Validating the AMRFinder tool and resistance gene database by using antimicrobial resistance genotype-phenotype correlations in a collection of isolates. Antimicrob Agents Chemother 63: e00483-19.

77. Jain C, Rodriguez-R LM, Phillippy AM, Konstantinidis KT, Aluru S (2018) High throughput ANI analysis of 90K prokaryotic genomes reveals clear species boundaries. Nat Commun 9: 5114.

Supporting information

S1 Fig. Comparison of the genome structure between strain 04Ya249 with 04Ya108, CAIM 1831 and TJ249. Structure comparison was performed using nucmer in MUMmer3 [74]. Purple dots indicate a match on the Watson strand (5’ to 3’ on the top strand in GenBank file), and light blue indicates a match on the Crick strand (5’ to 3’ on the bottom strand). (B) Average nucleotide identity (ANI) between two strains as determined by fastANI [77]. The commands used were as follows: (A) $nucmer -minmatch 60../../data/04Ya249_submission.fas../../data/reference.fas $mummerplot -x "[0,6000000]" -y "[0,22000000]" -postscript -p test out.delta; (B) $fastANI -q../../data/04Ya249_submission.fas -r../../data/CAIM1831_Refseq.fas -o 04Ya249vsCAIM1831.txt

879 $fastANI -q../../data/04Ya249_submission.fas -r../../data/04Ya108_submission.fas -o
880 04Ya249vs04Ya108.txt
881 $fastANI -q../../data/04Ya249_submission.fas -r../../data/04Ya108_submission.fas -o
882 04Ya249vs04Ya108.txt
883
884 **S2 Fig. Genetic map of pSEA2**. (A) Locations of antimicrobial resistance (AMR) genes and SE-
885 6945 in pSEA2. AMR genes were inferred using AMRFinderPlus [76]. Genes were visualized
886 using CLC Sequence Viewer (Qiagen, Hilden Germany). (B) Location of SEs in pSEA1 and
887 pSEA2. Four SE core genes are indicated by four distinct colors. Red pentagons are the β-
888 lactamase gene.
889
890 **S3 Fig. *attL* sequences formed in the SE-6945 integration regions.** Sequences are derived
891 from 04Ya249 genomes (AP019851.1, AP019849.1), TJ239 genome (*insJ*, *yjjNt*), and *Vibrio*
892 *harveri* strain WXL538 (CP045070.1) carrying a SE-6945-like element carrying a different set
893 of cargo genes. Sequences in red are incorporated into circular copy of SE. 6-bp underlined
894 sequence is incorporated into *attS* during SE circle formation. 19 bp motif C highlighted in
895 yellow form an imperfect inverted repeat with the motif C' located the other terminus of SE.
896 Sequence highlighted in cyan is a putative transcription termination motif. Asterisks indicate
897 conserved nucleotides.
898
899 **S4 Fig. *attR* sequences formed in the SE-6945 integration regions.** Sequences are derived
900 from 04Ya249 genomes (AP019851.1, AP019849.1), TJ239 genome (*insJ*, *yjjNt*), and *Vibrio*
901 *harveri* strain WXL538 (CP045070.1). Sequences in red are incorporated into circular copy of

SE. The 6 bp underlined sequences originate from the original *attB* or SE circle, and they are not incorporated into the *attS* of *the* SE circle.

S5 Fig. Inference of SE-6945 insertion number and its integration location by Southern hybridization. (A) *in silico* restriction map of DNA segments around SE-6945 integration locations in strain 04Ya249, TJ249, and a hypothetical *E. coli* strain carrying a pSEA2 insertion into SE-6945 integrated into *yjjNt*. Locations of SE-6945 and *intA* probe hybridization region are indicated by the yellow square and black filled square, respectively, above the restriction map. Horizontal black lines indicate the fragments detected by the probe and their sizes. (B) Southern blots of the pSEA2-free Vibrio strain LN95 and the parental strain 04Ya249. Genomic DNA was double digested with *NdeI* and *HindIII* (the left two lanes) or *NdeI* and *SphI* (the right two lanes). The probe used was 5' end of *intA*. Four unique bands originate from fragments shown in the first two rows (04Ya249 pSEA2, 04Ya249 chr1) in panel A. (C) Southern blots of 19 *E. coli* transconjugants obtained from 19 independent mating assays. Upper panel shows digestion with *NdeI* and *SphI*. Lower panel shows digestion with *NdeI* and *HindIII*. The color of the strain name indicates the pattern of SE/pSEA2 insertion deduced from restriction maps in panel A: blue, three SE copies (*yjjNt*::SE-6945, *insJ*::SE-6945::pSEA2); red, two SE copies (*insJ*::SE-6945::pSEA2); purple, (*yjjNt:*:SE-6945::pSEA2); lime, one SE copy (*yjjNt*::SE-6945 or chr::pSEA2); Strains with asterisk (*) are expected to carry pSEA2 in an unknown chromosomal location without generating a SE-6945-chromosome junction.

S6 Fig. *attL* sequences formed in the SE-6283 insertion regions. Sequences are derived from strain 04Ya108 (AP024165.1, AP024167.1), *E. coli* transconjugant TJ108W0 sequenced

in our previous study [30], and *Vibrio* strains carrying SE-6283-like elements listed in Fig 3. Sequences in red are incorporated into circular copy of SE. Incorporation of the 6 bp underlined sequence of TJ108W0 and pSEA1 into *attS* was demonstrated in the previous study.

S7 Fig. *attR* sequences formed in the SE-6283 insertion regions. Sequences are derived from genomes listed in Fig 3. Regarding SE-6283, the 6 bp underlined sequences in *attR* originate from inserting SE circle, and they are not incorporated into *attS* upon SE circularization.

S8 Fig. PCR detection of SE-6945 circle in *V. alfacsensis* strain 04Ya249 and *E. coli* strain LN52. (A) PCR detection of chromosomal *attL*, *attR*, *attS* in 04Ya249. (B) Relative copy number of *attS* in *V. alfacsensis* LN95 (no pSEA2). Copy number is represented as relative copy number to *gyrB*. Primers used are shown in Table 2. (C) PCR detection of *attS* in pSEA2 free *E. coli* strain LN52.

S1 Table. MIC of transconjugant strains

S2 Table. Data availability

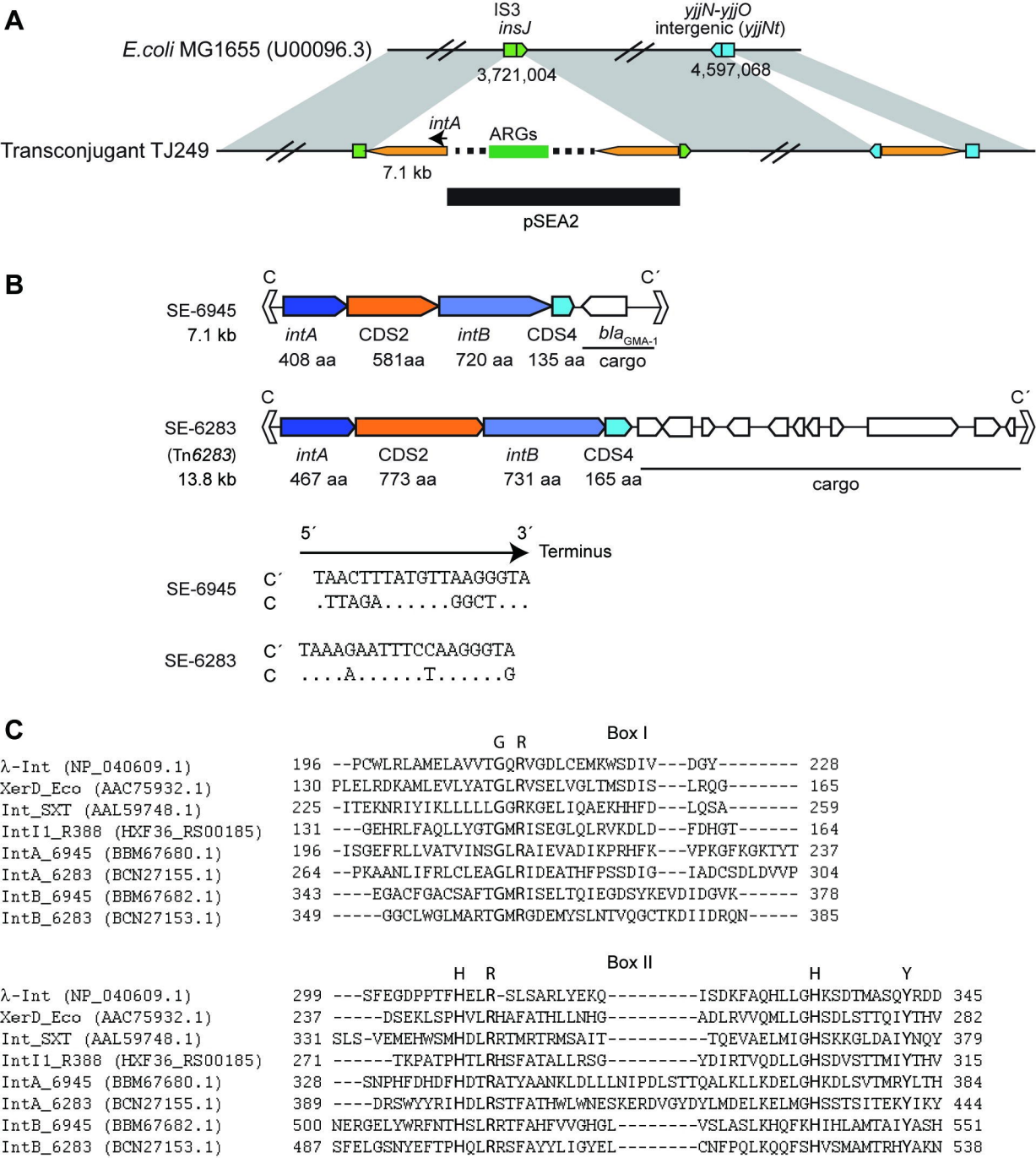
A
IS3
insJ
yjjN-yjjO
intergenic (yjjNt)
E.coli MG1655 (U00096.3)
3,721,004
4,597,068
intA
ARGs
Transconjugant TJ249
7.1 kb
pSEA2
B
C
C´
SE-6945
7.1 kb
intA
CDS2
intB
CDS4
bla GMA-1
408 aa
581aa
720 aa
135 aa
cargo
C
C´
SE-6283
(Tn6283)
13.8 kb
intA
CDS2
intB
CDS4
467 aa
773 aa
731 aa
165 aa
cargo
5´
3´
Terminus
SE-6945
C´ TAACTTTATGTTAAGGGTA
C .TTAGA.....GGCT...
SE-6283
C´ TAAAGAATTTCCAAGGGTA
C ....A.....T.....G
C
Box I
G R
λ-Int (NP_040609.1) 196 --PCWLRLAMELAVVTGQRVGDLCEMKWSDIV---DGY-------- 228
XerD_Eco (AAC75932.1) 130 PLELRDKAMLEVLYATGLRVSELVGLTMSDIS---LRQG------- 165
Int_SXT (AAL59748.1) 225 -ITEKNRIYIKLLLLLGGRKGELIQAEKHHFD---LQSA------- 259
IntI1_R388 (HXF36_RS00185) 131 ---GEHRLFAQLLYGTGMRISEGLQLRVKDLD---FDHGT------ 164
IntA_6945 (BBM67680.1) 196 -ISGEFRLLVATVINSGLRAIEVADIKPRHFK---VPKGFKGKTYT 237
IntA_6283 (BCN27155.1) 264 --PKAANLIFRLCLEAGLRIDEATHFPSSDIG---IADCSDLDVVP 304
IntB_6945 (BBM67682.1) 343 ----EGACFGACSAFTGMRISELTQIEGDSYKEVDIDGVK------ 378
IntB_6283 (BCN27153.1) 349 -----GGCLWGLMARTGMRGDEMYSLNTVQGCTKDIIDRQN----- 385
Box II
H R
H Y
λ-Int (NP_040609.1) 299 ---SFEGDPPTFHELR-SLSARLYEKQ---------ISDKFAQHLLGHKSDTMASQYRDD 345
XerD_Eco (AAC75932.1) 237 -----DSEKLSPHVLRHAFATHLLNHG---------ADLRVVQMLLGHSDLSTTQIYTHV 282
Int_SXT (AAL59748.1) 331 SLS-VEMEHWSMHDLRRTMRTRMSAIT----------TQEVAELMIGHSKKGLDAIYNQY 379
IntI1_R388 (HXF36_RS00185) 271 ------TKPATPHTLRHSFATALLRSG---------YDIRTVQDLLGHSDVSTTMIYTHV 315
IntA_6945 (BBM67680.1) 328 ---SNPHFDHDFHDTRATYAANKLDLLLNIPDLSTTQALKLLKDELGHKDLSVTMRYLTH 384
IntA_6283 (BCN27155.1) 389 ----DRSWYYRIHDLRSTFATHWLWNESKERDVGYDYLMDELKELMGHSSTSITEKYIKY 444
IntB_6945 (BBM67682.1) 500 NERGELYWRFNTHSLRRTFAHFVVGHGL--------VSLASLKHQFKHIHLAMTAIYASH 551
IntB_6283 (BCN27153.1) 487 SFELGSNYEFTPHQLRRSFAYYLIGYEL--------CNFPQLKQQFSHVSMAMTRHYAKN 538

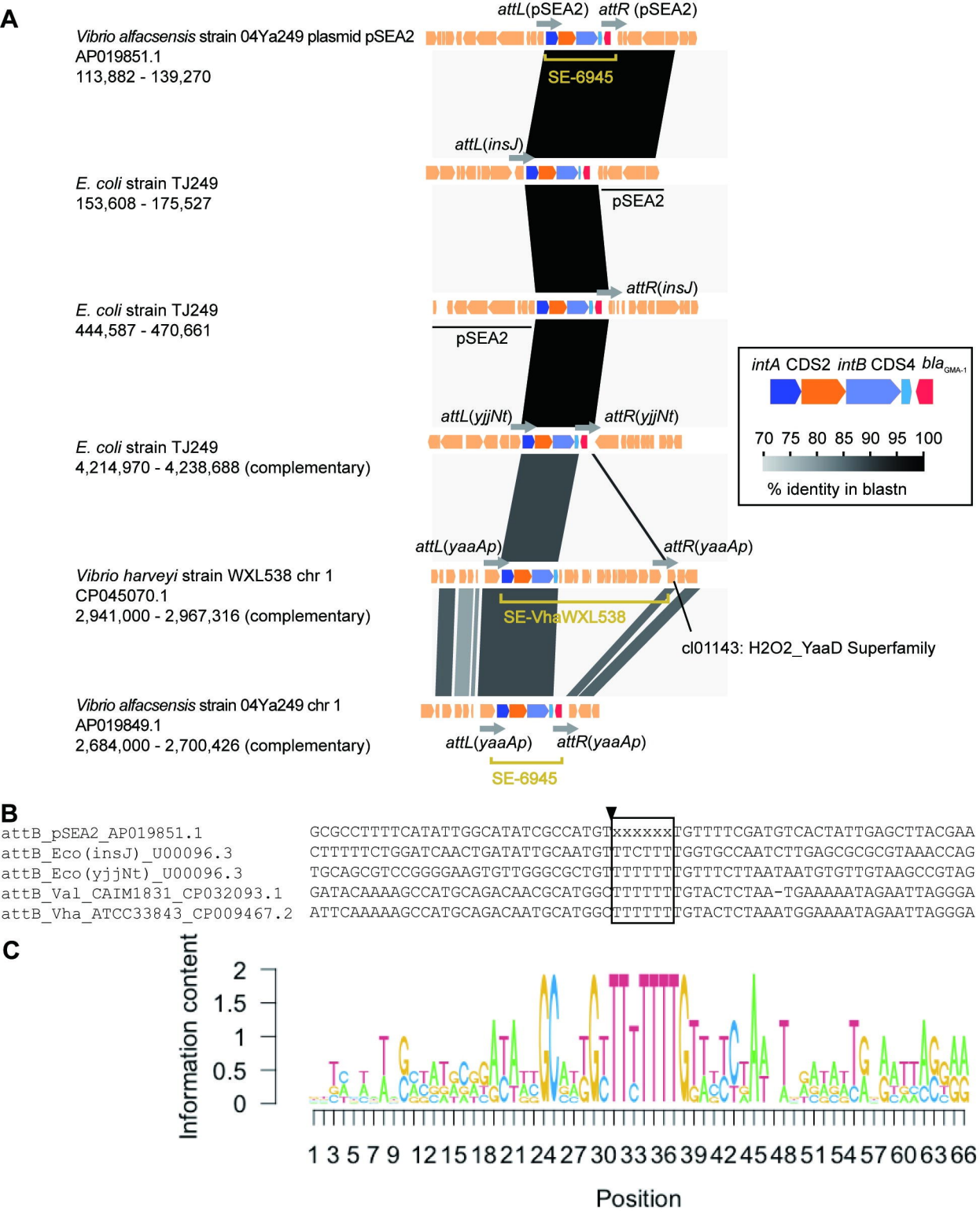
A
attL(pSEA2) attR (pSEA2)
Vibrio alfacsensis strain 04Ya249 plasmid pSEA2
AP019851.1
113,882 - 139,270
SE-6945
attL(insJ)
E. coli strain TJ249
153,608 - 175,527
pSEA2
attR(insJ)
E. coli strain TJ249
444,587 - 470,661
pSEA2
attL(yjjNt)
attR(yjjNt)
E. coli strain TJ249
4,214,970 - 4,238,688 (complementary)
attL(yaaAp)
attR(yaaAp)
Vibrio harveyi strain WXL538 chr 1
CP045070.1
2,941,000 - 2,967,316 (complementary)
SE-VhaWXL538
cl01143: H2O2_YaaD Superfamily
Vibrio alfacsensis strain 04Ya249 chr 1
AP019849.1
2,684,000 - 2,700,426 (complementary)
attL(yaaAp)
attR(yaaAp)
SE-6945
intA CDS2 intB CDS4 bla GMA-1
70 75 80 85 90 95 100
% identity in blastn
B
attB_pSEA2_AP019851.1 GCGCCTTTTCATATTGGCATATCGCCATGTxxxxxxTGTTTTCGATGTCACTATTGAGCTTACGAA
attB_Eco(insJ)_U00096.3 CTTTTTCTGGATCAACTGATATTGCAATGTTTCTTTTGGTGCCAATCTTGAGCGCGCGTAAACCAG
attB_Eco(yjjNt)_U00096.3 TGCAGCGTCCGGGGAAGTGTTGGGCGCTGTTTTTTTTGTTTCTTAATAATGTGTTGTAAGCCGTAG
attB_Val_CAIM1831_CP032093.1 GATACAAAAGCCATGCAGACAACGCATGGCTTTTTTTGTACTCTAA-TGAAAAATAGAATTAGGGA
attB_Vha_ATCC33843_CP009467.2 ATTCAAAAAGCCATGCAGACAATGCATGGCTTTTTTTGTACTCTAAATGGAAAATAGAATTAGGGA
C
Information content
2
1.5
1
0.5
0
1 3 5 7 9 12 15 18 21 24 27 30 33 36 39 42 45 48 51 54 57 60 63 66
Position

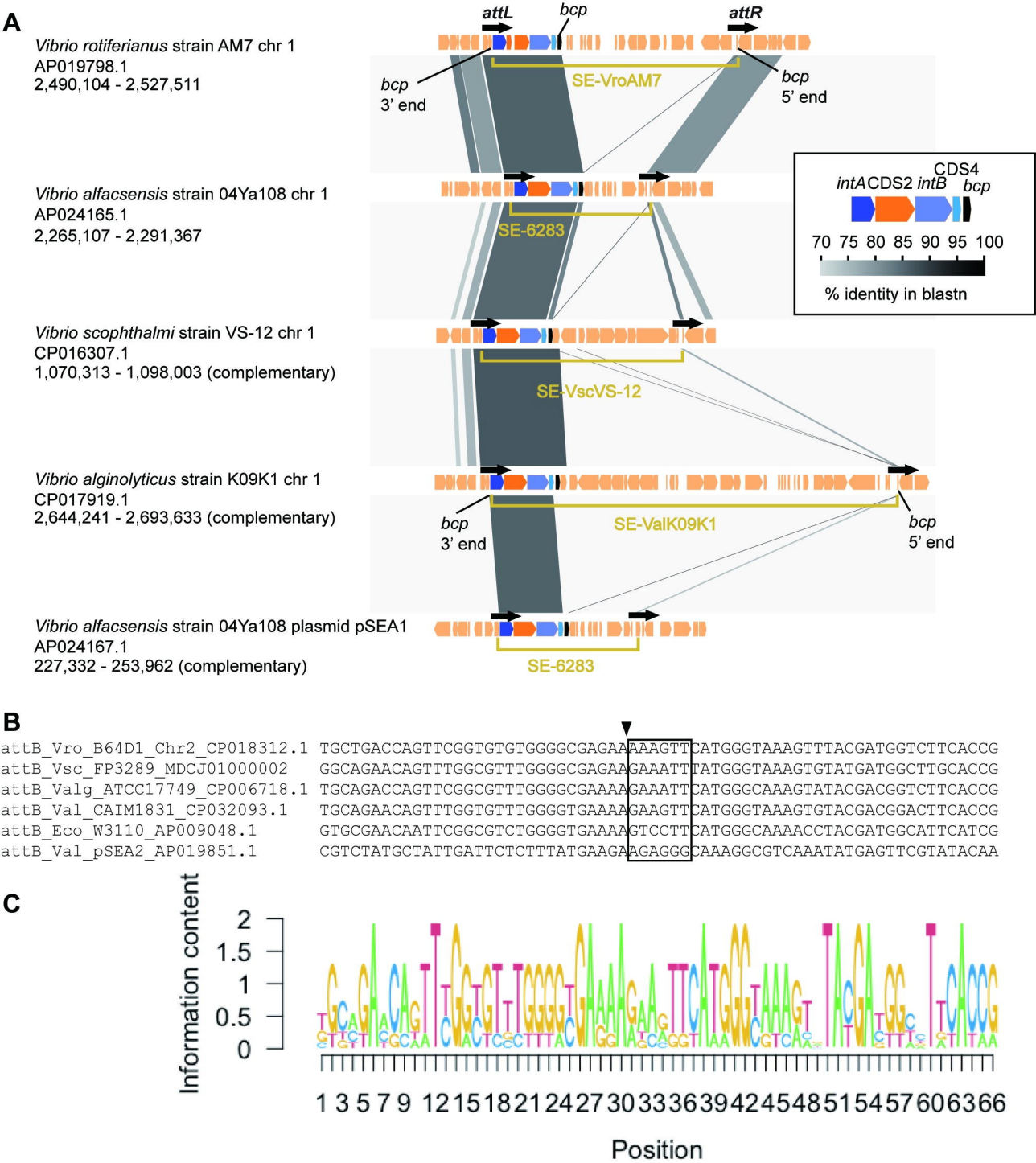
A
attL
bcp
attR
Vibrio rotiferianus strain AM7 chr 1
AP019798.1
2,490,104 - 2,527,511
bcp
3' end
SE-VroAM7
bcp
5' end
Vibrio alfacsensis strain 04Ya108 chr 1
AP024165.1
2,265,107 - 2,291,367
SE-6283
CDS4
intA CDS2 intB bcp
70 75 80 85 90 95 100
% identity in blastn
Vibrio scophthalmi strain VS-12 chr 1
CP016307.1
1,070,313 - 1,098,003 (complementary)
SE-VscVS-12
Vibrio alginolyticus strain K09K1 chr 1
CP017919.1
2,644,241 - 2,693,633 (complementary)
bcp
3' end
SE-ValK09K1
bcp
5' end
Vibrio alfacsensis strain 04Ya108 plasmid pSEA1
AP024167.1
227,332 - 253,962 (complementary)
SE-6283
B
attB_Vro_B64D1_Chr2_CP018312.1 TGCTGACCAGTTCGGTGTGTGGGGCGAGAAAAAGTTCATGGGTAAAGTTTACGATGGTCTTCACCG
attB_Vsc_FP3289_MDCJ01000002 GGCAGAACAGTTTGGCGTTTGGGGCGAGAAGAAATTTATGGGTAAAGTGTATGATGGCTTGCACCG
attB_Valg_ATCC17749_CP006718.1 TGCAGACCAGTTCGGCGTTTGGGGCGAAAAGAAATTCATGGGCAAAGTATACGACGGTCTTCACCG
attB_Val_CAIM1831_CP032093.1 TGCAGAACAGTTTGGTGTTTGGGGTGAAAAGAAGTTCATGGGTAAAGTGTACGACGGACTTCACCG
attB_Eco_W3110_AP009048.1 GTGCGAACAATTCGGCGTCTGGGGTGAAAAGTCCTTCATGGGCAAAACCTACGATGGCATTCATCG
attB_Val_pSEA2_AP019851.1 CGTCTATGCTATTGATTCTCTTTATGAAGAAGAGGGCAAAGGCGTCAAATATGAGTTCGTATACAA
C
Information content
2
1.5
1
0.5
0
1 3 5 7 9 12 15 18 21 24 27 30 33 36 39 42 45 48 51 54 57 60 63 66
Position

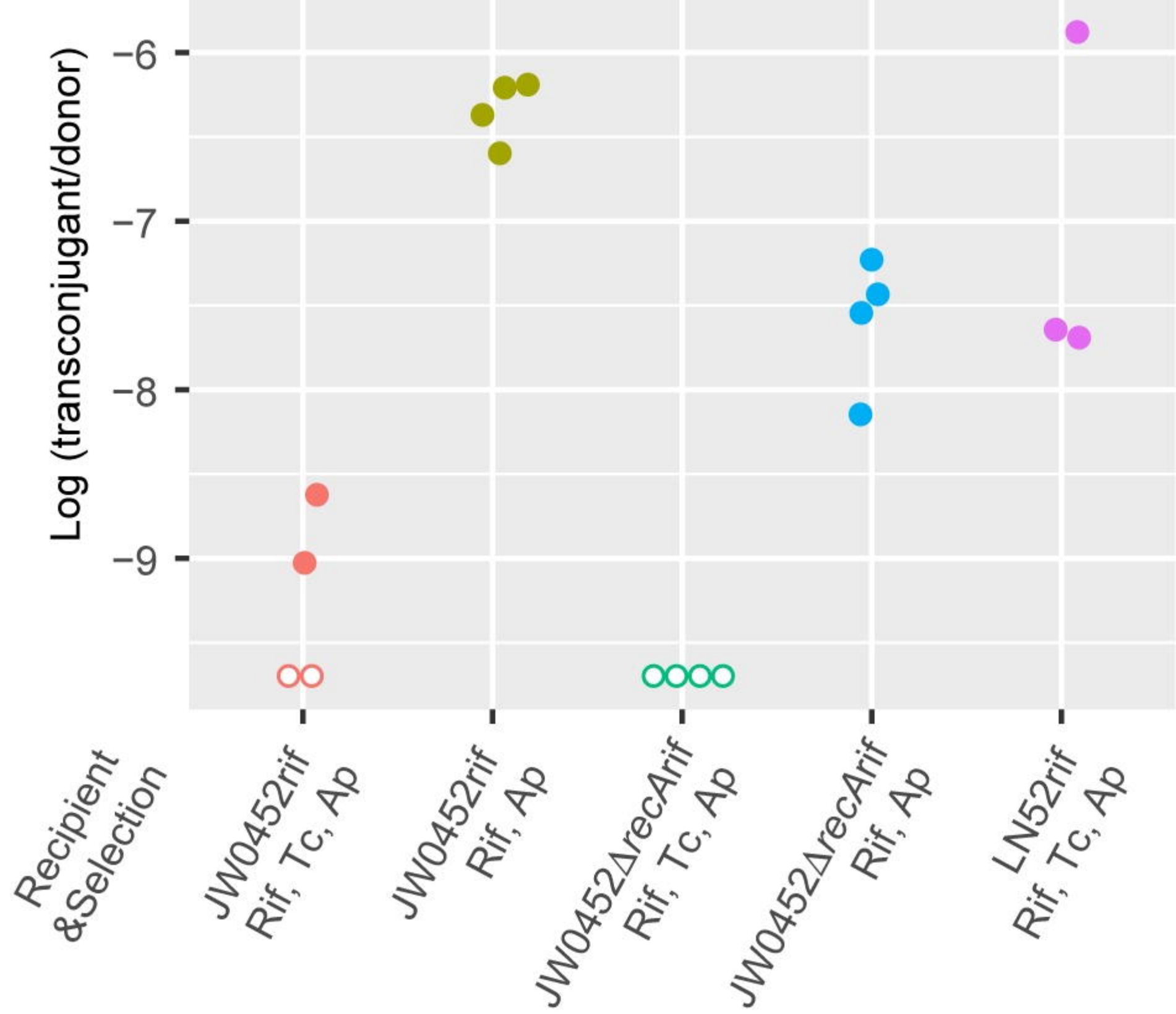
Log (transconjugant/donor)
−6
−7
−8
−9
Recipient &Selection
JW0452rif Rif, Tc, Ap
JW0452rif Rif, Ap
JW0452ΔrecArif Rif, Tc, Ap
JW0452ΔrecArif Rif, Ap
LN52rif Rif, Tc, Ap

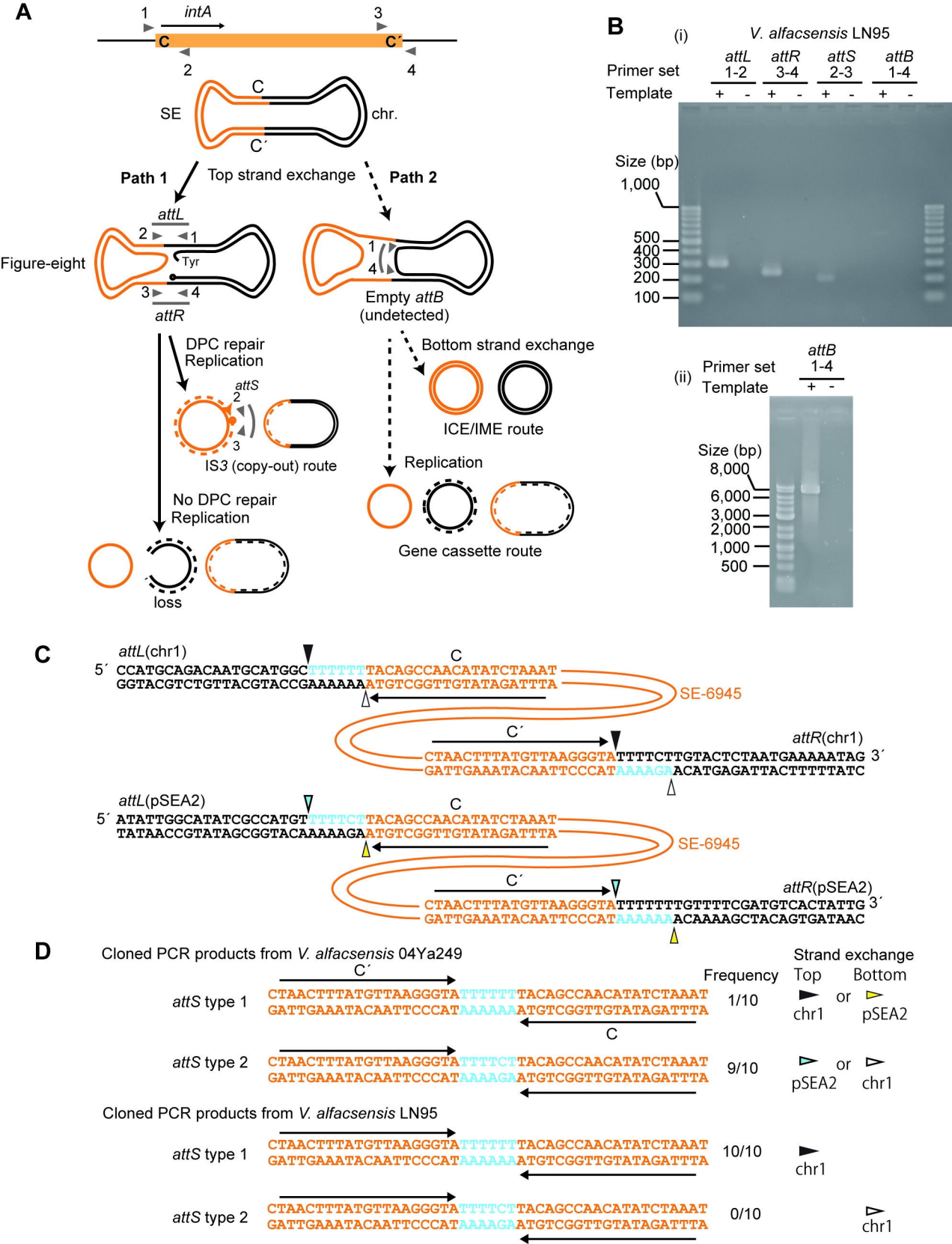
A
intA
1
2
3
4
C
C´
SE
chr.
Path 1
Top strand exchange
Path 2
attL
attR
Figure-eight
Tyr
Empty attB
(undetected)
DPC repair
Replication
attS
IS3 (copy-out) route
Bottom strand exchange
ICE/IME route
Replication
Gene cassette route
No DPC repair
Replication
loss
B
(i)
V. alfacsensis LN95
Primer set
attL 1-2
attR 3-4
attS 2-3
attB 1-4
Template
+ - + - + - + -
Size (bp)
1,000
500
400
300
200
100
(ii)
Primer set
attB 1-4
Template
+ -
Size (bp)
8,000
6,000
3,000
2,000
1,000
500
C
attL(chr1)
5´ CCATGCAGACAATGCATGGCTTTTTTTACAGCCAACATATCTAAAT
GGTACGTCTGTTACGTACCGAAAAAAATGTCGGTTGTATAGATTTA
SE-6945
C´
attR(chr1)
CTAACTTTATGTTAAGGGTATTTTCTTGTACTCTAATGAAAAATAG 3´
GATTGAAATACAATTCCCATAAAAGAACATGAGATTACTTTTTATC
attL(pSEA2)
5´ ATATTGGCATATCGCCATGTTTTTCTTACAGCCAACATATCTAAAT
TATAACCGTATAGCGGTACAAAAAGAATGTCGGTTGTATAGATTTA
SE-6945
C´
attR(pSEA2)
CTAACTTTATGTTAAGGGTATTTTTTTGTTTTCGATGTCACTATTG 3´
GATTGAAATACAATTCCCATAAAAAAACAAAAGCTACAGTGATAAC
D
Cloned PCR products from V. alfacsensis 04Ya249
Frequency
Strand exchange
Top
Bottom
attS type 1
CTAACTTTATGTTAAGGGTATTTTTTTACAGCCAACATATCTAAAT
GATTGAAATACAATTCCCATAAAAAAATGTCGGTTGTATAGATTTA
1/10
chr1
or
pSEA2
attS type 2
CTAACTTTATGTTAAGGGTATTTTCTTACAGCCAACATATCTAAAT
GATTGAAATACAATTCCCATAAAAGAATGTCGGTTGTATAGATTTA
9/10
pSEA2
or
chr1
Cloned PCR products from V. alfacsensis LN95
attS type 1
CTAACTTTATGTTAAGGGTATTTTTTTACAGCCAACATATCTAAAT
GATTGAAATACAATTCCCATAAAAAAATGTCGGTTGTATAGATTTA
10/10
chr1
attS type 2
CTAACTTTATGTTAAGGGTATTTTCTTACAGCCAACATATCTAAAT
GATTGAAATACAATTCCCATAAAAGAATGTCGGTTGTATAGATTTA
0/10
chr1

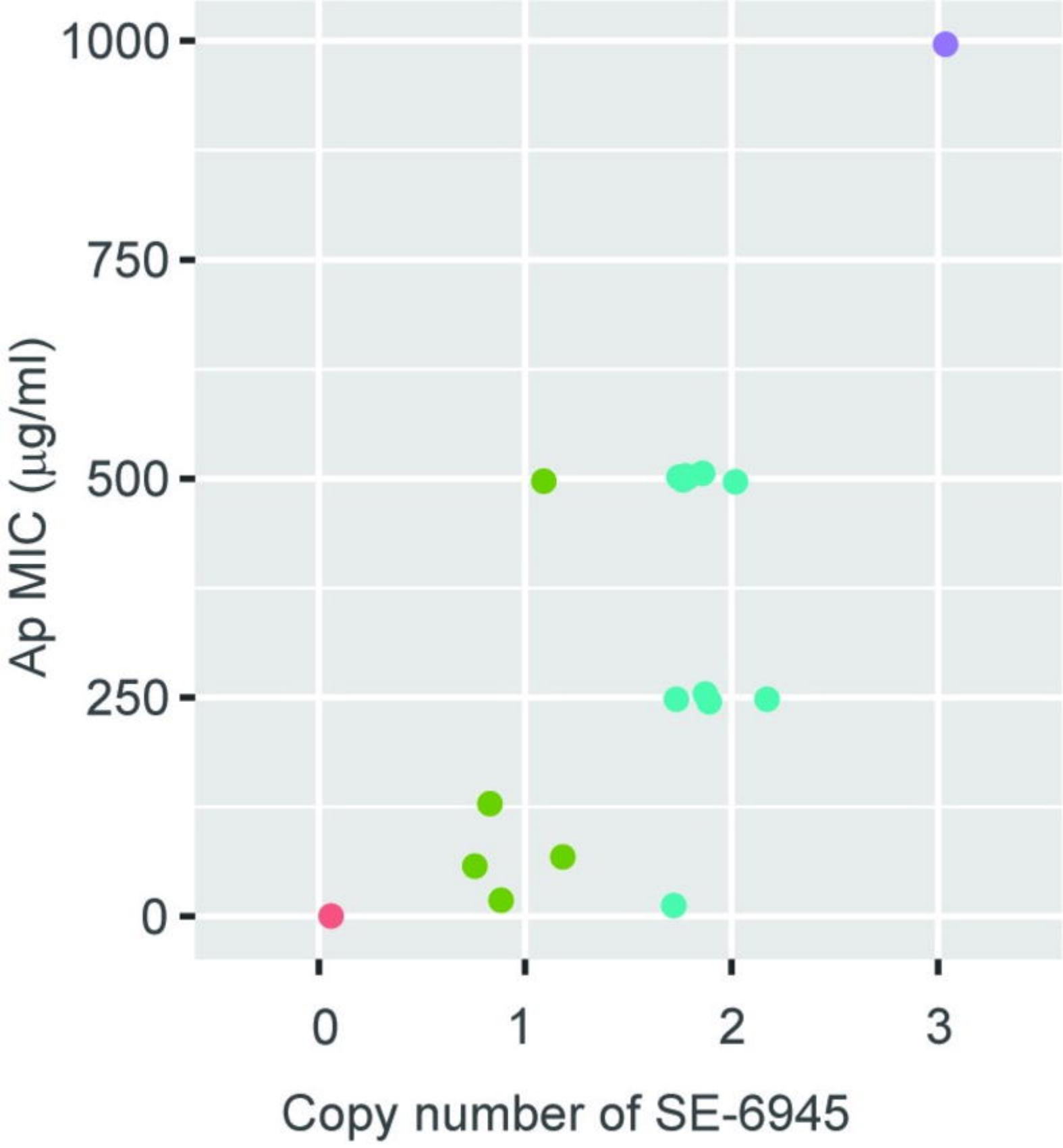
1000
750
500
250
0
Ap MIC (µg/ml)
0
1
2
3
Copy number of SE-6945